Int. J. Appl. Math. Comput. Sci., 2024, Vol. 34, No. 1, 45–64
DOI: 10.61822/amcs-2024-0004

A HIERARCHICAL OBSERVER FOR A NON–LINEAR UNCERTAIN CSTR MODEL OF BIOCHEMICAL PROCESSES

MATEUSZ CZYŻNIEWSKI [a], RAFAŁ ŁANGOWSKI [a,b,*]

[a]Department of Intelligent Control and Decision Support Systems
Gdańsk University of Technology
G. Narutowicza 11/12, 80-233 Gdańsk, Poland
e-mail: {mateusz.czyzniewski,rafal.langowski}@pg.edu.pl

[b]Digital Technologies Center
Gdańsk University of Technology
G. Narutowicza 11/12, 80-233 Gdańsk, Poland

The problem of estimation of unmeasured state variables and unknown reaction kinetic functions for selected biochemical processes modelled as a continuous stirred tank reactor is addressed in this paper. In particular, a new hierarchical (sequential) state observer is derived to generate stable and robust estimates of the state variables and kinetic functions. The developed hierarchical observer uses an adjusted asymptotic observer and an adopted super-twisting sliding mode observer. The stability of the proposed hierarchical observer is investigated under uncertainty in the system dynamics. The stability analysis of the estimation error dynamics is carried out based on the methodology associated with linear parameter-varying systems and sliding mode regimes. The developed hierarchical observer is implemented in the Matlab/Simulink environment and its performance is validated via simulation. The obtained satisfactory estimation results demonstrate high effectiveness of the devised hierarchical observer.

Keywords: bioreactors, hierarchical observers, non-linear uncertain systems, observers, state estimation.

1. Introduction

Urban water systems containing drinking water supply and distribution systems and water resource recovery facilities (WRRFs) are some of the most necessary systems for the functioning of a modern society. Efficient operation of these systems should be based on proper understanding of natural phenomena taking place in them and, at the same time, should be supported by advanced control and monitoring algorithms. These algorithms require current information about the state of a particular process (system), primarily passed from the measuring infrastructure installed at the plant. However, it is well known that many process variables, especially state ones, may be unmeasurable (Torfs *et al.*, 2022; Łangowski and Brdys, 2018; 2017; Junosza-Szaniawski *et al.*, 2022). In such situations, a state observer is employed, which makes it possible to estimate (reconstruct) state variables based on the knowledge of inputs to the plant, available measurements (measured outputs), as well as the knowledge of the system dynamics represented by its appropriate mathematical model. The system state estimation domain has been developed for many years, but there is room for improvement, especially concerning complex systems. The topic undertaken in this paper concerns the reconstruction of unmeasured state variables and unknown kinetic functions in WRRFs.

As mentioned above, a proper mathematical model of the biochemical processes considered is necessary for estimation purposes. Typically, this utility model can be developed using a mechanistic (white-box) approach, or by applying a data-driven (black-box) framework. In this paper, the first type of model is used. Two main groups of non-linear mechanistic models of biochemical processes occurring in WRRFs can be distinguished. These are activated sludge models (ASMs) and balance models (Bastin and Dochain, 1990; Dochain and Vanrolleghem, 2001; Henze *et al.*, 2000; Ujazdowski *et al.*, 2023). The ASM model family is perceived as most faithfully

*Corresponding author

reflecting the behaviour of natural processes in WRRFs. However, these models are characterised by a significant degree of complexity, and, therefore, it is not always possible to use them to synthesise a state observer. An alternative is to use models from the second group. The balance models are based on physical balance laws and aggregate certain fractions occurring in ASMs. The most common balance models are continuous stirred tank reactors (CSTRs). Unfortunately, a relatively simple structure of these models often entails the appearance of uncertainty, which is primarily accumulated in the kinetic function (growth rate function). In the broadest case, this function may be completely unknown (Bastin and Dochain, 1990; De Battista *et al*., 2011; Czyżniewski and Łangowski, 2022b).

In the context of developing an observer for biochemical processes modelled in this way at the WRRF, two main issues may be considered. Firstly, it is the reconstruction of (unmeasured) state variables in the presence of uncertainty, and, secondly, it is the estimation of an unknown kinetic function. Whereas the state variables are invoked for individual compounds residing in the WRRF bioreactor, the kinetic function is a crucial part of the dynamics responsible for shaping the overall process. Many types of observers can be found in the literature to reconstruct bioreactor state variables in the face of uncertainty. These include Luenberger-like observers (Bastin and Dochain, 1990; Dochain and Perrier, 2002; Bogaerts and Coutinho, 2014; Czyżniewski *et al*., 2023; López-Estrada *et al*., 2015), adaptive observers (Moshksar and Guay, 2014; Srinivasarengan *et al*., 2018; Rodríguez *et al*., 2015; Reis de Souza *et al*., 2020) together with Kalman filters (Dewasme *et al*., 2013; Bogaerts and Vande Wouwer, 2003; Bogaerts, 1999; Sun *et al*., 2008), high-gain observers (Bastin and Dochain, 1990; Dochain and Vanrolleghem, 2001; Lafont *et al*., 2014), interval observers (Hadj-Sadok and Gouzé, 2005; Alcaraz-González *et al*., 2005; Oubabas *et al*., 2018), moving- and full-horizon observers (Yin and Liu, 2017; Taylor *et al*., 2022; Elsheikh *et al*., 2021; Tuveri *et al*., 2022; Dewasme and Vande Wouwer, 2020; Bogaerts and Hanus, 2001; Hulhoven *et al*., 2008), asymptotic observers (Bastin and Dochain, 1990; Dochain and Vanrolleghem, 2001; Hadj-Sadok and Gouzé, 2005; Ha Hoang *et al*., 2013), and various types of sliding mode observers (Coutinho *et al*., 2019; Czyżniewski and Łangowski, 2022b; De Battista *et al*., 2012; López-Caamal and Moreno, 2016; Nuñez *et al*., 2013; Czyżniewski *et al*., 2023; Fridman *et al*., 2011). Moreover, many solutions combining different estimation techniques can be found, i.e., the so-called hybrid observers (Bogaerts and Coutinho, 2014; Bogaerts and Vande Wouwer, 2003; Oubabas *et al*., 2018; Hulhoven *et al*., 2006; Lemesle and Gouzé, 2005; Rueda-Escobedo *et al*., 2022; Bárzaga-Martell *et al*., 2021; Ríos *et al*., 2018; López-Caamal and Moreno, 2016). It is worth adding that many of the observers mentioned above reveal the robustness property. Robustness means the ability to reject the effects of uncertainties by, e.g., using the interval approach, appropriate transformation of the state coordinates, or fine-tuning the algorithm parameters. Moreover, this property is often associated with the possibility of direct reconstruction of unknown inputs (disturbances) and parameters.

This work focuses on developing and combining the asymptotic and sliding mode approaches. This is because the structure of the asymptotic observer (AO) allows the elimination of the unknown kinetic function by transforming the state vector, which leads to the reconstruction of the unmeasured state variables. However, the AO requires explicit knowledge of the input and does not have any tunable correction terms (Bastin and Dochain, 1990; Dochain and Vanrolleghem, 2001; Hadj-Sadok and Gouzé, 2005; Ha Hoang *et al*., 2013). On the other hand, the sliding mode observer, in the second-order variant called a super-twisting sliding mode observer (STSMO), allows exact estimation of the unknown kinetic function in the finite-time horizon and offers robustness against noise and discretization (Fridman *et al*., 2011; De Battista *et al*., 2012). However, the STSMO requires the knowledge of an adequate number of measurements. Utilising the advantages of the above two techniques while adapting the AO and STSMO to multiple input signals, and exploiting additional information (pseudo-measurements) have made it possible to propose a new hierarchical (sequential) observer.

The main aim of this work is to provide a new hierarchical observer that allows the estimation of both unmeasured state variables and unknown kinetic function in a separate manner. In detail, an adjusted AO enables the reconstruction of the unmeasured state variables independently of the impact of the kinetic function. In turn, an adopted STSMO allows the estimation of the unknown kinetic function based on both direct measurements and AO-generated estimates called pseudo-measurements. A certain class of CSTR-type models was used as a model of the biochemical processes occurring in the WRRF for estimation purposes. The performance of the developed hierarchical observer was simulation-verified in the Matlab/Simulink environment. To summarise, the main contributions of this paper are as follows:

- A new hierarchical observer producing asymptotically stable estimates of the unmeasured state variables and the unknown kinetic function is devised for the non-linear uncertain CSTR model of biochemical processes.
- New proofs of asymptotic convergence of the

estimates of the unmeasured state variables generated by the asymptotic observer and the estimates of the unknown kinetic function generated by the super-twisting sliding mode observer are derived.

- A comprehensive simulation analysis, including scenarios for various measured outputs, is presented.

The paper is organised as follows. The problem is formulated in Section 2, while Section 3 includes the synthesis of the asymptotic observer and the super twisting sliding mode observer, together forming the hierarchical observer. In Section 4, the case study is presented, with division into detailed observer design and the obtained simulation results. The paper is concluded in Section 5 and completed with Appendix.

2. Problem formulation

From the constituent mass balance law, a model of biochemical processes occurring in a bioreactor can be viewed as an n-dimensional multiple-input single-output (MISO) system belonging to a sub-class of the general class of affine non-linear dynamic systems. Let us consider a model of this type describing a certain class of CSTRs, which can be defined as follows (Khalil, 2002; Dochain and Vanrolleghem, 2001; Bastin and Dochain, 1990):

$$\Sigma_{\mathrm{G}}\colon \begin{cases} \dot{X}(t) = \mu(t)X(t) - m_{\mathrm{x}}X(t) \\ \qquad -(1+r)X(t)D(t) + rX_{\mathrm{r}}(t)D(t), \\ \dot{X}_{\mathrm{r}}(t) = v(1+r)X(t)D(t) \\ \qquad -v(w+r)X_{\mathrm{r}}(t)D(t), \\ \dot{\phi}_{j_{\mathrm{n}}}(t) = -Y_{j_{\mathrm{n}}}^{-1}\mu(t)X(t) - m_{j_{\mathrm{n}}}X(t) \\ \qquad +\phi_{j_{\mathrm{n}}}^{\mathrm{in}}(t)D(t) - (1+r)\phi_{j_{\mathrm{n}}}(t)D(t) \\ \qquad +Q_{j_{\mathrm{n}}}(t), \\ X(t_0) = X_0,\ X_{\mathrm{r}}(t_0) = X_{\mathrm{r},0}, \\ \phi_{j_{\mathrm{n}}}(t_0) = \phi_{j_{\mathrm{n}},0}, \\ j_{\mathrm{n}} = \overline{1, n-2}, \end{cases} \tag{1}$$

where $\dot{(\cdot)}$ stands for the derivative with respect to t; $t \in \mathbb{T} = \mathbb{R}_+$ is the time instant; $\mathbb{R}_+$ denotes the positive part of $\mathbb{R}$; $X(t)$ [mg/L] $\in \mathbb{R}_+$, $X_{\mathrm{r}}(t)$ [mg/L] $\in \mathbb{R}_+$, and $\phi_{j_{\mathrm{n}}}(t)$ [mg/L] $\in \mathbb{R}_+$ are the concentrations of aggregated biomass, aggregated recirculated biomass, and the j_{n}-th (aggregated) non-biomass compound, respectively, with initial conditions X_0, $X_{\mathrm{r},0}$ and $\phi_{j_{\mathrm{n}},0}$; $\mu(t)$ [h^{-1}] $\in \mathbb{W} \subset \mathbb{R}_+$ signifies the kinetic function (growth rate function); $D(t) = Q_{\mathrm{in}}(t)/V_{\mathrm{a}}$ [h^{-1}] $\in \mathbb{R}_+$ is the dilution rate, where $Q_{\mathrm{in}}(t)$ [m^3/h] $\in \mathbb{R}_+$ and V_{a} [m^3] $\in \mathbb{R}_+$ are the inflow rate to the bioreactor and its volume, respectively; $\phi_{j_{\mathrm{n}}}^{\mathrm{in}}(t)$ [mg/L] $\in \mathbb{R}_+$ stands for the concentration of a given compound in inflow to the bioreactor; $Q_{j_{\mathrm{n}}}(t)$ [mg/h L] $\in \mathbb{R}_+$ is the gas-liquid transfer rate of the j_{n}-th non-biomass compound; m_{x} [h^{-1}] $\in \mathbb{R}_+$ denotes the biomass mortality rate; $m_{j_{\mathrm{n}}}$ [h^{-1}] $\in \mathbb{R}_+$ signifies the maintenance coefficient for the j_{n}-th non-biomass compound; $Y_{j_{\mathrm{n}}}$ [$-$] $\in \mathbb{R}_+$ denotes the yield coefficient for the j_{n}-th non-biomass compound; $r = Q_{\mathrm{r}}(t)/Q_{\mathrm{in}}(t)$ [$-$] $\in \mathbb{R}_+$ is the constant proportion between the rates of inflow and recirculated flow, where $Q_{\mathrm{r}}(t)$ [m^3/h] $\in \mathbb{R}_+$ is the recirculated flow rate; $v = V_{\mathrm{a}}/V_{\mathrm{s}}$ [$-$] $\in \mathbb{R}_+$ denotes the constant proportion between the bioreactor and settler volumes, where V_{s} [m^3] $\in \mathbb{R}_+$ is the settler volume; and $w = Q_{\mathrm{w}}(t)/Q_{\mathrm{in}}(t)$ [$-$] $\in \mathbb{R}_+$ stands for the constant proportion between the rates of wastewater flow and inflow, where $Q_{\mathrm{w}}(t)$ [m^3/h] $\in \mathbb{R}_+$ is the wastewater flow rate.

Assumption 1. The vector of state variables of the model (1) is defined as $\boldsymbol{x}(t) \in \mathbb{R}_+^{\mathrm{n}}$. More specifically, the vector of the state variables is proposed as

$$\boldsymbol{x}(t) \triangleq \begin{bmatrix} X(t) & \phi_{j_{\mathrm{n}}}(t) & X_{\mathrm{r}}(t) \end{bmatrix}^{\mathrm{T}}.$$

Assumption 2. By their nature, in operational conditions all variables and parameters in the model (1) are positive and uniformly bounded. For further discussion, $\forall t \in \mathbb{T}$ the set of all possible system states, is defined as (Dochain and Vanrolleghem, 2001; Bastin and Dochain, 1990)

$$\mathbb{X}_{\mathrm{n}} = \left\{ \forall t \in \mathbb{T},\ \boldsymbol{x}(t) \in \mathbb{R}_+^{\mathrm{n}} : \underline{\boldsymbol{x}} \preceq \boldsymbol{x}(t) \preceq \overline{\boldsymbol{x}} \right\},$$

where $\underline{(\cdot)}$ and $\overline{(\cdot)}$ signify the real and positive lower and upper bounds on the particular variable, and $\preceq$ refers to element-wise operations between the laid-out elements of a given vector or matrix. $\mathbb{X}_{\mathrm{n}}$ is the invariant set known with the condition of the general theory of dynamics of biochemical processes.

Assumption 3. Only one state variable is transferred to the system output, i.e., $y(t) \in \mathbb{Y}_{\mathrm{q}} \subset \mathbb{R}_+$, and it represents the measured output, hence $y(t) = h(\boldsymbol{x}(t)) = C\boldsymbol{x}(t)$, where $\boldsymbol{C} \in \mathbb{R}^{1\times \mathrm{n}}$ is the output matrix.

Assumption 4. In the operational conditions, the inputs to the model (1) are defined as $\boldsymbol{u}(t) \in \mathbb{U}_{\mathrm{p}} \subset \mathbb{R}^{\mathrm{p}}$:

$$\boldsymbol{u}(t) \triangleq \begin{bmatrix} D(t) & D(t)\phi_{j_{\mathrm{n}}}^{\mathrm{in}}(t) & k_{\mathrm{L}}a_{j_{\mathrm{n}}}(t) \end{bmatrix}^{\mathrm{T}},$$

$$\mathbb{U}_{\mathrm{p}} = \left\{ \forall t \in \mathbb{T},\ \boldsymbol{u}(t) \in \mathbb{R}_+^{\mathrm{p}} : \underline{\boldsymbol{u}} \preceq \boldsymbol{u}(t) \preceq \overline{\boldsymbol{u}} \right\}.$$

Vector $\boldsymbol{u}(t)$ is the vector of time-dependent functions, which are at least $\boldsymbol{u}(t) \in \mathcal{C}^1(\mathbb{T}, \mathbb{U}_{\mathrm{p}})$ uniformly bounded Lipschitz continuous functions. Let us define $\|\cdot\|_\infty$ for the supremum norm (Shilov and Chilov, 1996); then $\forall t \in \mathbb{T}$: $\left\|\dot{u}_{i_{\mathrm{p}}}(t)\right\|_\infty = \sup\left\{ |\ \dot{u}_{i_{\mathrm{p}}}\ | :\ t \in \mathbb{T} \right\} \leq \overline{u}_{\mathrm{d}_{i_{\mathrm{p}}}} < \infty$ for $i_{\mathrm{p}} = \overline{1, p}$. Moreover, due to the physical properties

of the system considered, it is assumed that all inputs are the permanently excited positive signals, i.e., $\forall t \in \mathbb{T}$; the following matrix is bounded and positive definite (Khalil, 2002; Jenkins *et al*., 2018):

$$\underline{\alpha}_{\mathrm{u}} \boldsymbol{I}_{(\mathrm{p}\times\mathrm{p})} \leqslant \int_{t}^{T+t} \boldsymbol{u}(\tau)\boldsymbol{u}^{\mathrm{T}}(\tau)\,\mathrm{d}\tau \leqslant \overline{\alpha}_{\mathrm{u}} \boldsymbol{I}_{(\mathrm{p}\times\mathrm{p})}\ ,$$

where $\leqslant$ refers to the domination order of the particularly definite matrices; $\underline{\alpha}_{\mathrm{u}}$ and $\overline{\alpha}_{\mathrm{u}} \in \mathbb{R}_{+}$ are the constant parameters; $T \in \mathbb{T}$ is the selected time period; and $\boldsymbol{I}_{((\cdot)\times(\cdot))}$ is the identity matrix of the appropriate size.

Assumption 5. The model of the gas-liquid transfer rate of the j_{n}-th non-biomass compound that describes direct transfer between gas and liquid surroundings, e.g., the oxygen transfer rate from the gas phase to the liquid phase and the carbon transfer rate from the liquid phase to the gas phase (Dewasme *et al*., 2013; Lindberg, 1997; Dochain and Vanrolleghem, 2001; Bastin and Dochain, 1990), yields

$$Q_{j_{\mathrm{n}}}(t) \triangleq k_{\mathrm{L}} a_{j_{\mathrm{n}}}(t)\left(\phi_{j_{\mathrm{n}}}^{\mathrm{sat}} - \phi_{j_{\mathrm{n}}}(t)\right),$$

where $k_{\mathrm{L}}a_{j_{\mathrm{n}}}(t)\ [\mathrm{h}^{-1}] \in \mathbb{R}_{+}$ is the particular gas-liquid transfer function and $\phi_{j_{\mathrm{n}}}^{\mathrm{sat}}\ [\mathrm{mg/L}] \in \mathbb{R}_{+}$ is the saturation concentration of the j_{n}-th non-biomass compound.

It is worth emphasising that $k_{\mathrm{L}}a_{j_{\mathrm{n}}}(t)$ can be viewed not only as an input modelled in various ways, but also as a time-varying parameter (Lindberg, 1997; Piotrowski *et al*., 2021; Dewasme *et al*., 2019; Czyżniewski *et al*., 2023).

Assumption 6. By their nature, in the operational conditions all parameters in the model (1), i.e., m_{x}, $m_{j_{\mathrm{n}}}$, $Y_{j_{\mathrm{n}}}$, r, v, w and $\phi_{j_{\mathrm{n}}}^{\mathrm{sat}}$, are positive and assumed known and constant (Dochain and Vanrolleghem, 2001; Bastin and Dochain, 1990).

Assumption 7. It is assumed here that the kinetic function $\mu(t)$ is unknown and thus introduces uncertainty alone into the model (1). However, due to the physical understanding of distinctive biochemical processes, it is possible to impose the following properties on this function (Czyżniewski and Łangowski, 2022b; Dochain and Vanrolleghem, 2001):

- $\mu(t)$ is always non-negative and uniformly bounded, i.e., $\forall t \in \mathbb{T}\colon\ \|\mu(t)\|_{\infty} = \sup\{|\ \mu(t)\ |\colon\ t \in \mathbb{T}\} \leq \overline{\mu} < \infty$;
- $\mu(t)$ is always the Lipschitz continuous function of its arguments, which means that its derivative is also uniformly bounded, i.e., $\forall t \in \mathbb{T}\colon\ \|\dot{\mu}(t)\|_{\infty} = \sup\{|\ \dot{\mu}(t)\ |\colon\ t \in \mathbb{T}\} \leq \overline{\mu}_{\mathrm{d}} < \infty$.

Proposition 1. *For the sake of simplicity, according to Assumptions 1–4, the model* (1) *can be rewritten in the following way:*

$$\begin{cases} \dot{\boldsymbol{\mathcal{X}}}(t) = \boldsymbol{\mathcal{R}}\mu(t)x_1(t) - \boldsymbol{\varphi}x_1(t) - (1+r)\boldsymbol{\mathcal{X}}(t)u_1(t) \\ \qquad\qquad +\boldsymbol{Q}(t) + \boldsymbol{\zeta}(t) + \boldsymbol{s}(t), \\ \dot{x}_n(t) = v(1+r)x_1(t)u_1(t) - v(w+r)x_n(t)u_1(t), \\ y(t) = \boldsymbol{C}\boldsymbol{x}(t), \\ \boldsymbol{x}(t_0) = \boldsymbol{x}_0, \end{cases} \tag{2}$$

where $\boldsymbol{\mathcal{X}}(t) = \begin{bmatrix} x_1(t) & \dots & x_{n-1} \end{bmatrix}^{\mathrm{T}} \in \mathbb{R}_{+}^{\mathrm{n}-1}$ *is the reduced state vector;* $\boldsymbol{\mathcal{R}} = \begin{bmatrix} 1 & -Y_{j_{\mathrm{n}}} \end{bmatrix}^{\mathrm{T}} \in \mathbb{R}_{+}^{\mathrm{n}-1}$ *stands for the vector of yield coefficients;* $\boldsymbol{Q}(t) = \begin{bmatrix} 0 & Q_{j_{\mathrm{n}}}(t) \end{bmatrix}^{\mathrm{T}} \in \mathbb{R}_{+}^{\mathrm{n}-1}$ *denotes the vector of gas-liquid inflow/outflow rates;* $\boldsymbol{\varphi} = \begin{bmatrix} m_{\mathrm{x}} & m_{j_{\mathrm{n}}} \end{bmatrix}^{\mathrm{T}} \in \mathbb{R}_{+}^{\mathrm{n}-1}$ *signifies the vector of mortality and maintenance coefficients;* $\boldsymbol{\zeta}(t) = \begin{bmatrix} 0 & \zeta_2(\boldsymbol{u}(t)) & \dots & \zeta_{n-1}(\boldsymbol{u}(t)) \end{bmatrix}^{\mathrm{T}} \in \mathbb{R}_{+}^{\mathrm{n}-1}$ *is the vector of combined inputs;* $\boldsymbol{s}(t) = \begin{bmatrix} rx_n(t)u_1(t) & 0 & \dots & 0 \end{bmatrix}^{\mathrm{T}} \in \mathbb{R}_{+}^{\mathrm{n}-1}$ *denotes the vector describing the relation between the recirculated biomass and other compounds; and* $j_{\mathrm{n}} = \overline{1, n-2}$.

It is noteworthy that the introduced structure (2) fits into the general structure of biochemical systems (Bastin and Dochain, 1990; Dochain and Vanrolleghem, 2001).

Remark 1. It is worth emphasising that the CSTR class represented by the models (1) and (2) may be easily transformed to the fed batch form known from, e.g., the works of Dochain and Vanrolleghem (2001), Bastin and Dochain (1990), Moreno and Dochain (2008), López-Caamal and Moreno (2016) or Bogaerts and Coutinho (2014). In this regard, it is necessary to make $r = 0$, which cancels the impact of the concentration of the recirculated biomass (or other concentrations of the recirculated compounds) in these models.

As mentioned above, the main goal of this work is developing a robust hierarchical observer for biochemical systems belonging to the class described by the model (2). The robustness property is related to the estimation of the unmeasured state variables and the unknown kinetic function in a global asymptotic way. This is done by applying a sequential structure of two separate observers responsible for independent estimation tasks, where the AO allows the reconstruction of the unmeasured state variables irrelevant of how the kinetic function behaves, while the STSMO uses a simplified model of the process to assess the unknown value of $\mu(t)$ with the assumption that the upper bound on the kinetic function derivative is known. This operation is performed when there is only one state measurement and the knowledge about the inputs enabling to provide the u-detectability property of the state (Czyżniewski and Łangowski, 2022a;

Moreno and Dochain, 2008; Moreno *et al*., 2012). Since the developed STSMO used to estimate $\mu(t)$ gets the information from both the measured output and the pseudo-measurements, which are the AO-related estimates of state variables, the global asymptotic stability of the entire structure must be proved by utilising the Lyapunov tools. This is the main difference between this study and the previous works (e.g., Bastin and Dochain, 1990; López-Caamal and Moreno, 2016; Dochain and Vanrolleghem, 2001; De Battista *et al*., 2011; Farza *et al*., 1998; Dewasme *et al*., 2019; Rueda-Escobedo *et al*., 2022; Nuñez *et al*., 2013; Moshksar and Guay, 2014), where only direct measurements were applied to reconstruct the kinetic function, but more detailed knowledge on its structure was required. The proposed hierarchical approach adopts less restrictive assumptions about the number of direct measurements and the properties of the utility model for synthesis purposes. It is noteworthy that the estimation process is not parallel, unlike in other hybrid approaches (e.g., Bogaerts, 1999; Bogaerts and Coutinho, 2014; Oubabas *et al*., 2018; Hulhoven *et al*., 2006; Lemesle and Gouzé, 2005; Rueda-Escobedo *et al*., 2022; Bárzaga-Martell *et al*., 2021). Instead, it is executed in two steps, with one observer receiving the input from the other through a feed-forward connection. In this case, the pseudo-measurements provide additional information; however, their use may affect the STSMO performance due to longer transient states.

3. Synthesis of the hierarchical observer

The structure of the proposed hierarchical observer is shown in Fig. 1, where the flow of signals and causal dependencies between its particular parts are marked. According to Fig. 1, the estimation process is realised sequentially. An adjusted asymptotic observer allowing multiple inputs to be taken into account is used to reconstruct the unmeasured state variables, whereas the super-twisting sliding mode observer estimates the unknown kinetic function based on not only direct measurements of CSTR inputs and outputs but also the computed state estimates (pseudo-measurements) generated by the AO.

3.1. Design of an asymptotic observer. A well-known approach to designing an asymptotic observer for CSTR state reconstruction purposes is based on using the dilution rate $D(t)$ as the input to the dynamics observer (Dochain and Vanrolleghem, 2001; Bastin and Dochain, 1990; Hadj-Sadok and Gouzé, 2005; Ha Hoang *et al*., 2013). In this paper, the vector of inputs is extended by $k_{\mathrm{L}}a_{j_{\mathrm{n}}}(t)$ and $D(t)\phi^{\mathrm{in}}_{j_{\mathrm{n}}}(t)$, which makes the synthesis of the observer more challenging.

Proposition 2. *For such conditions, it is possible to select one k-th element, where $k \in \{1,\dots,n-1\}$, from the n-dimensional state vector $\boldsymbol{x}(t)$, except for $x_n(t)$, which is the measured output $y(t)$ (according to Assumption 3). Thus, the $(n-1)$-dimensional vector $\boldsymbol{v}(t) \in \mathbb{V}_{\mathrm{n-1}} \in \mathbb{R}^{\mathrm{n-1}}_{+}$ of unmeasured state variables can be introduced as part of vector $\boldsymbol{x}(t)$ by excluding a particular $x_k(t)$ variable. Next, to decline the unknown kinetic function $\mu(t)$ (see Assumption 7) from the system dynamics, a new vector of state variables $\boldsymbol{c}(t) \in \mathbb{G}_{\mathrm{n-1}} \in \mathbb{R}^{\mathrm{n-1}}$ is introduced in the following way:*

$$\boldsymbol{c}(t) = \begin{cases} \boldsymbol{v}(t) + \boldsymbol{K}y(t) & \text{if} \quad y(t) \neq x_1(t), \\ \mathbf{1}_{(\mathrm{n-1})\times 1}y(t) + \boldsymbol{F}\boldsymbol{v}(t) & \text{if} \quad y(t) = x_1(t), \end{cases}$$

$$\boldsymbol{K} = \begin{bmatrix} R_k^{-1} & -\dfrac{R_\kappa}{R_k} & 0 \end{bmatrix}^{\mathrm{T}}$$

$$\text{if } k \in \{2,\dots,n-1\}, \quad \kappa = \overline{1, n-1} \setminus \{k\},$$

$$\boldsymbol{F} = \operatorname{diag}\left(\begin{bmatrix} R_2^{-1} & \dots & R_{n-1}^{-1} & 1 \end{bmatrix}^{T}\right) \quad \text{if } k = 1,$$

where $\mathbf{1}_{(\mathrm{n-1})\times 1}$ is the vector consisting of elements equal to 1 excluding the element associated with $x_n(t)$ while $\boldsymbol{K} \in \mathbb{R}^{\mathrm{n-1}}$, $\boldsymbol{F} \in \mathbb{R}^{(\mathrm{n-1})\times(\mathrm{n-1})}$ are, respectively, the matrix and vector of coordinate transformations that consist of the particular yield coefficients determined in vector $\boldsymbol{\mathcal{R}}$.

Given the transformation from Proposition 2, the model (2) can be rewritten as

$$\Sigma_{\mathrm{c}} \begin{cases} \dot{\boldsymbol{c}}(t) = \boldsymbol{A}(\boldsymbol{u}(t))\boldsymbol{c}(t) + \boldsymbol{B}(y(t), \boldsymbol{u}(t)), \\ \boldsymbol{c}(t_0) = \boldsymbol{c}_0, \end{cases} \tag{3}$$

where $\boldsymbol{A}(\boldsymbol{u}(t))\colon \mathbb{U}_{\mathrm{p}} \to \mathbb{R}^{\mathrm{n\times n}}$ is the time-varying matrix of differentiable functions representing the internal dynamics of the system, while $\boldsymbol{B}(y(t), \boldsymbol{u}(t))\colon \mathbb{Y}_{\mathrm{q}} \times \mathbb{U}_{\mathrm{p}} \to \mathbb{R}^{\mathrm{n}}$ denotes the time-varying vector of differentiable functions related to inputs and the measured output.

The derivation of $\boldsymbol{A}(\boldsymbol{u}(t))$ and $\boldsymbol{B}(y(t), \boldsymbol{u}(t))$ is premised on an appropriate composition of components $\boldsymbol{s}(t)$, $\boldsymbol{Q}(t)$, $\boldsymbol{\mathcal{R}}$, $\boldsymbol{\zeta}(t)$, $\boldsymbol{\varphi}$, $\boldsymbol{\mathcal{X}}(t)$ and $x_n(t)$ introduced in Proposition 1. Specifically, it is done by applying the state coordinate transformation from Proposition 2. Taking into account that the $\mu(t)$ related term has been eliminated from the new dynamics and only linear or bi-linear dependencies between particular signals and parameters occur, particular elements of $\boldsymbol{A}(\boldsymbol{u}(t))$ and $\boldsymbol{B}(y(t), \boldsymbol{u}(t))$ can be obtained.

Remark 2. Whereas the form of vector $\boldsymbol{B}\left(y(t), \boldsymbol{u}(t)\right)$ is fully dependent on linear or non-linear combinations of parameters with inputs $\boldsymbol{u}(t)$ and the measured output $y(t)$, the form of matrix $\boldsymbol{A}\left(\boldsymbol{u}(t)\right)$ is based on combinations between parameters and inputs. For comparison, in a typical approach to AO design, the matrix responsible for the internal dynamics depends only on parameters.

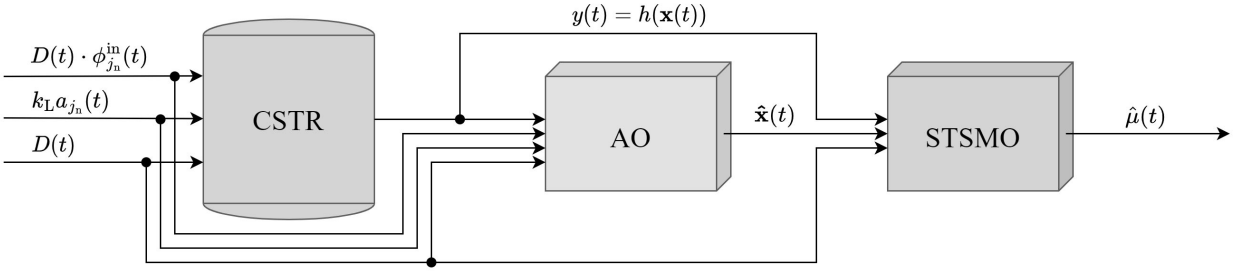

Fig. 1. Diagram of the proposed hierarchical observer.

Therefore, this new representation of system dynamics must be viewed as a linear parameter-varying system (LPV).

Lemma 1. *To design the asymptotic observer, the following conditions must hold:*

1. *The elements of vector* $\boldsymbol{K}$ *must satisfy* $K_l \neq 0$, $l = \overline{1, n-2}$, *excluding the last element, i.e.,* $l = n-1$ *if* $y(t) \neq x_1(t)$.
2. *The rank of diagonal matrix* $\boldsymbol{F}$ *must meet* $\operatorname{rank}(\boldsymbol{F}) = n-1$, *if* $y(t) = x_1(t)$.
3. *The rank of matrix* $\boldsymbol{A}(\boldsymbol{u}(t))$ *must meet* $\operatorname{rank}(\boldsymbol{A}(\boldsymbol{u}(t))) = n-1, \forall t \in \mathbb{T}$.

The impact of the measured output $y(t)$ on the modelled dynamics (3) decoupled from $\mu(t)$ can be directly considered to be stabilising. Hence, the vector of unmeasured state variables $\boldsymbol{v}(t)$ may be reconstructed in an asymptotic way by the asymptotic observer.

Theorem 1. *Assuming that vector* $\boldsymbol{c}(t)$ *represents the solution of the system* (3) *over time* $t \in \mathbb{T}$ *and denoting by* $\hat{\boldsymbol{c}}(t) \in \mathbb{G}_{n-1} \in \mathbb{R}^{n-1}$ *and* $\hat{\boldsymbol{v}}(t) \in \mathbb{V}_{n-1} \in \mathbb{R}_{+}^{n-1}$ *the estimates of state variables, the following asymptotic observer:*

$$\Sigma_{\text{AO}}: \begin{cases} \dot{\hat{\boldsymbol{c}}}(t) = \boldsymbol{A}(\boldsymbol{u}(t))\,\hat{\boldsymbol{c}}(t) + \boldsymbol{B}(y(t), \boldsymbol{u}(t)), \\ \hat{\boldsymbol{v}}(t) = \hat{\boldsymbol{c}}(t) - \boldsymbol{K} y(t), \\ \hat{\boldsymbol{c}}(t_0) = \hat{\boldsymbol{c}}_0, \end{cases} \tag{4}$$

or

$$\Sigma_{\text{AO}}: \begin{cases} \dot{\hat{\boldsymbol{c}}}(t) = \boldsymbol{A}(\boldsymbol{u}(t))\,\hat{\boldsymbol{c}}(t) + \boldsymbol{B}(y(t), \boldsymbol{u}(t)), \\ \hat{\boldsymbol{v}}(t) = \boldsymbol{F}^{-1}\left[\hat{\boldsymbol{c}}(t) - \boldsymbol{1}_{(n-1)\times 1} y(t)\right], \\ \hat{\boldsymbol{c}}(t_0) = \hat{\boldsymbol{c}}_0 \end{cases}$$

generates the estimates of state variables $\hat{\boldsymbol{x}}(t)$ *asymptotically (exponentially) converging to the state vector* $\boldsymbol{x}(t)$ *of the system* (1) *as* $t \to \infty$ *for any initial conditions and any permanently excited vector* $\boldsymbol{u}(t)$.

Proof. By combining (3) and (4), the dynamics of the estimation error $\boldsymbol{e}(t) \triangleq \hat{\boldsymbol{c}}(t) - \boldsymbol{c}(t) \in \mathbb{E}_{n-1} \subset \mathbb{R}^{n-1}$ are given as

$$\Sigma_{\text{e}}: \begin{cases} \dot{\boldsymbol{e}}(t) = \boldsymbol{A}(\boldsymbol{u}(t))\,\boldsymbol{e}(t), \\ \boldsymbol{e}(t_0) = \boldsymbol{e}_0. \end{cases} \tag{5}$$

Referring to, e.g., Khalil (2002), Ilchmann *et al.* (1987) or Zhou (2016), the LPV dynamics (5) can be considered to be globally and asymptotically (exponentially) stable (GAES) if and only if the following conditions hold:

1. The real parts of all eigenvalues of matrix $\boldsymbol{A}(\boldsymbol{u}(t))$ are negative, i.e., $\forall t \in \mathbb{T}$: $\lambda_{j_n}[\boldsymbol{A}(\boldsymbol{u}(t))] \subset \{z \in \mathbb{C} | \Re(z) < 0\}$, where z is the complex number and $\Re(\cdot)$ denotes the real part of the complex number z.
2. Matrix $\boldsymbol{A}(\boldsymbol{u}(t))$ is uniformly bounded, i.e., $\forall t \in \mathbb{T}$: $\|\boldsymbol{A}(\boldsymbol{u}(t))\|_2 \leq \gamma$.
3. The time derivative $\dot{\boldsymbol{A}}(\boldsymbol{u}(t))$ is uniformly bounded, i.e., $\forall t \in \mathbb{T}$: $||\dot{\boldsymbol{A}}(\boldsymbol{u}(t))||_2 \leq \delta$;.

Here $\delta, \gamma \in \mathbb{R}_{+}$ are the constant parameters.

If the conditions presented in Lemma 1 are met and the input vector $\boldsymbol{u}(t)$ is permanently excited (see Assumption 4), then the GAES property of the proposed AO related to the estimation error equilibrium zero point is assured for every $\boldsymbol{e}(t_0) = \boldsymbol{e}_0$ in the classic way, i.e.,

$$\boldsymbol{\Phi}(t, t_0) = \exp\left(\int_{t_0}^{t} \boldsymbol{A}(\boldsymbol{u}(\tau))\,\mathrm{d}\tau\right),$$

$$\|\boldsymbol{\Phi}(t, t_0)\|_2 \leq \eta_1 \exp\left(-\eta_2 (t - t_0)\right),$$

$$\boldsymbol{e}(t) = \boldsymbol{\Phi}(t, t_0)\boldsymbol{e}(t_0) \to \boldsymbol{0}_{(n-1)} \text{ as } t \to \infty,$$

where $\boldsymbol{\Phi}(t, t_0): \mathbb{T} \to \mathbb{G}_{n-1}$ denotes the state transition matrix of the LPV system and η_1, $\eta_2 \in \mathbb{R}_{+}$ are the positive constant parameters.

The justification of the second and the third condition is based on the fact that the input $\boldsymbol{u}(t)$ and its derivatives $\dot{\boldsymbol{u}}(t)$ are uniformly bounded and continuous, which is guaranteed by Assumptions 2–4. Additionally, since matrix $\boldsymbol{A}(\boldsymbol{u}(t))$ is the differentiable function with respect

to $\boldsymbol{u}(t)$ (see Remark 2), there exist uniformly bounded and continuous partial derivatives $\partial_{\boldsymbol{u}}\boldsymbol{A}\left(\boldsymbol{u}(t)\right)$ (for a detailed discussion of this issue, see Appendix).

The final part of the stability proof is performed in the same manner as in the works of Khalil (2002) and Ilchmann *et al*. (1987), hence only necessary stages are presented here. To show that the trajectories of the estimation error converge to the zero equilibrium point, the quadratic radially unbounded Lyapunov function $\mathcal{V}_{\mathrm{A}}\left(\boldsymbol{e}(t),t\right):\mathbb{E}_{\mathrm{n}-1}\times\mathbb{T}\to\mathbb{R}_{+}\cup\{0\}$ is proposed:

$$\begin{aligned}&\mathcal{V}_{\mathrm{A}}\left(\boldsymbol{e}(t),t\right)\\&\quad=\boldsymbol{e}^{\mathrm{T}}(t)\boldsymbol{\mathcal{P}}_{\mathrm{A}}(t)\boldsymbol{e}(t),\ \underline{\lambda}\left(\boldsymbol{\mathcal{P}}_{\mathrm{A}}(t)\right)\left\|\boldsymbol{e}(t)\right\|_2^2\\&\quad\leq\mathcal{V}_{\mathrm{A}}\left(\boldsymbol{e}(t),t\right)\leq\overline{\lambda}\left(\boldsymbol{\mathcal{P}}_{\mathrm{A}}(t)\right)\left\|\boldsymbol{e}(t)\right\|_2^2,\end{aligned}\tag{6}$$

where $\boldsymbol{\mathcal{P}}_{\mathrm{A}}(t)\colon\mathbb{T}\to\mathbb{R}^{(\mathrm{n}-1)\times(\mathrm{n}-1)}$ is the real, positive definite and time dependent symmetric matrix, and $\overline{\lambda}\left(\boldsymbol{\mathcal{P}}_{\mathrm{A}}(t)\right)\in\mathbb{R}_{+}$ and $\underline{\lambda}\left(\boldsymbol{\mathcal{P}}_{\mathrm{A}}(t)\right)\in\mathbb{R}_{+}$ denote the largest and smallest eigenvalues of $\boldsymbol{\mathcal{P}}_{\mathrm{A}}(t)\ \forall t\in\mathbb{T}$, respectively.

Assuming that there exists a real, positive-definite and symmetric matrix $\boldsymbol{\mathcal{Q}}_{\mathrm{A}}(t)\colon\mathbb{T}\to\mathbb{R}_{+}^{(n-1)\times(n-1)}$ meeting the condition of uniform boundedness, i.e.,

$$\begin{aligned}\boldsymbol{0}_{(n-1)\times(n-1)}&\leqslant\underline{\sigma}\boldsymbol{I}_{(n-1)\times(n-1)}\\&\leqslant\boldsymbol{\mathcal{Q}}_{\mathrm{A}}(t)\leqslant\overline{\sigma}\boldsymbol{I}_{(n-1)\times(n-1)},\quad\forall t\in\mathbb{T},\end{aligned}$$

where $\underline{\sigma},\overline{\sigma}\in\mathbb{R}_{+}$, the Lyapunov equation is fulfilled by $\boldsymbol{\mathcal{P}}_{\mathrm{A}}(t)$ in the following way:

$$\begin{aligned}\boldsymbol{\mathcal{P}}_{\mathrm{A}}(t)&=\int_{\mathbb{T}}\left(\boldsymbol{\Phi}^{\mathrm{T}}(\tau,t_0)\boldsymbol{\mathcal{Q}}_{\mathrm{A}}(\tau)\boldsymbol{\Phi}(\tau,t_0)\right)\mathrm{d}\tau,\\-\dot{\boldsymbol{\mathcal{P}}}_{\mathrm{A}}(t)&=\boldsymbol{\mathcal{P}}_{\mathrm{A}}(t)\boldsymbol{A}(\boldsymbol{u}(t))+\boldsymbol{A}^{\mathrm{T}}(\boldsymbol{u}(t))\boldsymbol{\mathcal{P}}_{\mathrm{A}}(t)+\boldsymbol{\mathcal{Q}}_{\mathrm{A}}(t)\\&=\boldsymbol{A}(\boldsymbol{u}(t))\int_{\mathbb{T}}\left(\boldsymbol{\Phi}^{\mathrm{T}}(\tau,t_0)\boldsymbol{\mathcal{Q}}_{\mathrm{A}}(\tau)\boldsymbol{\Phi}(\tau,t_0)\right)\mathrm{d}\tau\\&\quad+\boldsymbol{A}^{\mathrm{T}}(\boldsymbol{u}(t))\int_{\mathbb{T}}\left(\boldsymbol{\Phi}^{\mathrm{T}}(\tau,t_0)\boldsymbol{\mathcal{Q}}_{\mathrm{A}}(\tau)\boldsymbol{\Phi}(\tau,t_0)\right)\mathrm{d}\tau\\&\quad+\boldsymbol{\mathcal{Q}}_{\mathrm{A}}(t).\end{aligned}\tag{7}$$

By combining (5), (6) and (7), the time derivative of $\mathcal{V}_{\mathrm{A}}\left(\boldsymbol{e}(t),t\right)$ is given as

$$\begin{aligned}\dot{\mathcal{V}}_{\mathrm{A}}\left(\boldsymbol{e}(t),t\right)&=\dot{\boldsymbol{e}}^{\mathrm{T}}(t)\boldsymbol{\mathcal{P}}_{\mathrm{A}}(t)\boldsymbol{e}(t)\\&\quad+\boldsymbol{e}^{\mathrm{T}}(t)\dot{\boldsymbol{\mathcal{P}}}_{\mathrm{A}}(t)\boldsymbol{e}(t)+\boldsymbol{e}^{\mathrm{T}}(t)\boldsymbol{\mathcal{P}}_{\mathrm{A}}(t)\dot{\boldsymbol{e}}(t)\\&=-\boldsymbol{e}^{\mathrm{T}}(t)\boldsymbol{\mathcal{Q}}_{\mathrm{A}}(t)\boldsymbol{e}(t).\end{aligned}\tag{8}$$

Therefore, taking into account that $||\boldsymbol{A}(\boldsymbol{u}(t))||_2\leq\gamma$ and $||\dot{\boldsymbol{A}}\left(\boldsymbol{u}(t)\right)||_2\leq\delta,\ \forall t\in\mathbb{T}$, the rest of the proof can be performed canonically (for more details, see (Khalil, 2002, pp. 147–159)), which guarantees the GAES property of dynamics (5). To sum up, knowing that the vector of the original state variables $\boldsymbol{x}(t)$ is combined by $y(t)$ and $\boldsymbol{v}(t)$, the full information about the system state is ensured and Theorem 1 is proven. ■

Remark 3. According to Moreno and Dochain (2008) as well as López-Caamal and Moreno (2016), the feasibility condition of the 'classic' AO is not involved with fulfilling the strong u-observability property, but only the less restrictive property of strong u-detectability, which arises from both the dynamics and the observer structure attributes. This means that, if the feasibility condition is satisfied, then any additional analysis of system observability is unnecessary for both the 'classic' and the proposed AO, which results from the global asymptotic convergence of the estimation error (5) dynamics to the zero point.

3.2. Design of the super-twisting sliding mode observer. By invoking Fig. 1, the modified super-twisting sliding mode observer known from De Battista *et al*. (2012) can be applied to the estimation of an unknown kinetic function. This is because the biomass-related concentration dynamics introduced in model (1) neatly fit the general form of the model presented by De Battista *et al*. (2012); see Remark 1.

In fact, the unknown kinetic function $\mu(t)$ is generally an uncertain and complex component of the dynamics of biochemical processes, whose non-linear behaviour depends on particular compound concentrations, pH, temperature, or other environmental factors (Czyżniewski *et al.*, 2023; De Battista *et al.*, 2012; 2011; Bastin and Dochain, 1990; Dochain and Vanrolleghem, 2001). Thus, by taking the first dynamics equation from the model (1), the proportional biomass representation of the kinetic function is applied:

$$\Sigma_{\mathrm{X}}\colon\begin{cases}\dot{X}(t)=\mu(t)X(t)-m_{\mathrm{x}}X(t)\\\qquad\quad-(1+r)D(t)X(t)+rD(t)X_{\mathrm{r}}(t),\\\dot{\mu}(t)=\rho(t)X(t),\\X(t_0)=X_0,\quad\mu(t_0)=\mu_0,\end{cases}\tag{9}$$

where $\rho(t)\colon\mathbb{T}\to\mathbb{R}$ is the unknown function uniformly bounded by the known constant $\overline{\rho}$, i.e., $\forall t\in\mathbb{T}\colon|\rho(t)|\leq\overline{\rho}\in\mathbb{R}_{+}$ (see Assumption 7), which describes the dynamic behaviour of the kinetic function $\mu(t)$.

Assumption 8. Any solution, understood in the sense of Filipov (Khalil, 2002), of the $\mu(t)$ related dynamics (9) satisfies the differential inclusion $\dot{\mu}(t)\in U\overline{\rho}X(t),\ \forall t\in\mathbb{T}$, where the convex set U is given as $U=[-1\ ,\ 1]\in\mathbb{R}$.

In contrast to De Battista *et al*. (2012), the proposed STSMO uses not only direct measurements of inputs to the CSTR, and outputs from the CSTR but also pseudo-measurements. Hence, the main issue is to

show that the structure (9) can be efficiently united with the proposed AO (4) when the pseudo-measurements 'play the role' of real measurements. Consequently, the global asymptotic stability of the estimation error in the finite time horizon (uniform stability), i.e., at time $t_0 < T_{\text{reach}} \in \mathbb{T}$, must be converted to the GAES property. Taking into account the form of the $X(t)$ related differential equation (1), the following cases can be considered:

1. The output given by $y(t) = X(t)$ is measured, whereas the estimate $\widehat{X}_{\text{r}}(t)$ of $X_{\text{r}}(t)$ stands for pseudo-measurement.
2. The estimates $\widehat{X}(t)$ and $\widehat{X}_{\text{r}}(t)$ of $X(t)$ and $X_{\text{r}}(t)$, respectively, signify pseudo-measurements.

Hence, by taking the $X(t)$ related dynamics equation from the model (1) and defining a new signal $\check{X}(t) \in \mathbb{R}_+$ as the universal indication representing both $X(t)$ and $\widehat{X}(t)$, regardless of the case, the following theorem is formulated.

Theorem 2. *Let a pair of* $(X(t), \mu(t))$, $\forall t \in \mathbb{T}$, *represent the part of the solution of the system* (1)*, understood in the sense of Filipov, with respect to the biomass concentration and kinetic function. Moreover, let us assume that the measurements and pseudo-measurements are available in the two particular cases. Then, the following super-twisting sliding mode observer:*

$$\Sigma_{\text{STSMO}}\colon \begin{cases} \dot{\hat{X}}(t) = r\widehat{X}_{\text{r}}(t)D(t) + \big(\hat{\mu}(t) \\ \qquad -m_{\text{x}} - (1+r)D(t)\big)\check{X}(t) \\ \qquad +2\beta\big[\overline{\rho}\big|\check{X}(t) - \hat{X}(t)\big|\big]^{0.5} \\ \qquad \times\text{sgn}\left(\check{X}(t) - \hat{X}(t)\right)\check{X}(t), \\ \dot{\hat{\mu}}(t) = \alpha\overline{\rho}\text{sgn}\big(\check{X}(t) - \hat{X}(t)\big)\check{X}(t), \\ \hat{X}(t_0) = \hat{X}_0,\ \hat{\mu}(t_0) = \hat{\mu}_0, \end{cases} \tag{10}$$

where $\alpha, \beta \in \mathbb{R}_+$ *are the tuning parameters and* $\text{sgn}(\cdot)$ *signifies the signum function, generates the estimate of the kinetic function* $\hat{\mu}(t)$ *asymptotically (exponentially) converging to the kinetic function* $\mu(t)$ *(GAES property) if the tuning parameters meet* $\alpha \in (1\,;\,\infty) \subset \mathbb{R}_+$ *and* $\beta \in \mathbb{R}_+$*, and* $\overline{\rho}$ *is properly calculated, for any initial conditions.*

Lemma 2. *Based on Assumptions 2, 4 and 7, the following properties are introduced:*

- *The AO related estimation error* $e_{\text{X}}(t) \triangleq X(t) - \check{X}(t) \in \mathbb{R}$*, which, due to the introduced properties of the AO (see Section 3.1), is GAES, i.e.,* $|e_{\text{X}}(t)| \to 0$ *as* $t \to \infty$*, and uniformly bounded, i.e.,* $\forall t \in \mathbb{T}\colon\ |e_{\text{X}}(t)| \le \overline{e_{\text{X}}} = \big|X(t_0) - \check{X}(t_0)\big| \in \mathbb{R}_+$*. Moreover, if* $\check{X}(t) \equiv X(t)$*, i.e.,* $y(t) = x_1(t)$*, then* $e_{\text{X}}(t) = 0$, $\forall t \in \mathbb{T}$.
- *The AO related estimation error,* $e_{\text{X}_{\text{r}}}(t) \triangleq X_{\text{r}}(t) - \widehat{X}_{\text{r}}(t) \in \mathbb{R}$ *reveals the same properties as* $e_{\text{X}}(t)$*, i.e., is GAES and uniformly bounded, i.e.,* $\forall t \in \mathbb{T}\colon\ |e_{\text{X}_{\text{r}}}(t)| \le \overline{e_{\text{X}_{\text{r}}}} = \big|X_{\text{r}}(t_0) - \widehat{X}_{\text{r}}(t_0)\big| \in \mathbb{R}_+$.
- *The estimation errors of the STSMO denoted as* $\tilde{X}(t) \triangleq X(t) - \hat{X}(t) \in \mathbb{R}$ *and* $\tilde{\mu}(t) \triangleq \mu(t) - \hat{\mu}(t) \in \mathbb{R}$ *are, at least, uniformly bounded, i.e.,* $\forall t \in \mathbb{T}\colon\ \big|\tilde{X}(t)\big| \le \tilde{X}_{\text{b}} \in \mathbb{R}_+$, $|\tilde{\mu}(t)| \le \tilde{\mu}_{\text{b}} \in \mathbb{R}_+$*, where both bounds are taken conservatively.*

Proof. Taking into account that the pseudo-measurements may 'supply' the correction term of the STSMO, the classic Lyapunov method-based stability analysis has to be invoked and reconsidered (De Battista *et al*., 2011; Nuñez *et al*., 2013; Moreno and Osorio, 2012; Moreno and Mendoza, 2014; Moreno, 2012). The proof of stability can be given by taking the fundamental properties of the proposed AO (4) and the STSMO (10) into account.

By combining the first differential equation from (1), the model (9), and Assumption 8 with the observer equations (10), the following error dynamics are obtained

$$\begin{cases} \dot{\tilde{X}}(t) = \tilde{\mu}(t)\check{X}(t) \\ \qquad +\big[\mu(t) - m_{\text{x}} - (1+r)D(t)\big]e_{\text{X}}(t) \\ \qquad +rD(t)e_{\text{X}_{\text{r}}}(t) - 2\beta\big[\overline{\rho}\big|\check{X}(t) - \hat{X}(t)\big|\big]^{0.5} \\ \qquad \times\text{sgn}\left(\check{X}(t) - \hat{X}(t)\right)\check{X}(t), \\ \dot{\tilde{\mu}}(t) \in U\overline{\rho}X(t) - \alpha\overline{\rho}\text{sgn}\big(\check{X}(t) - \hat{X}(t)\big)\check{X}(t), \\ \tilde{X}(t_0) = \tilde{X}_0,\ \tilde{\mu}(t_0) = \tilde{\mu}_0. \end{cases} \tag{11}$$

It can be noticed that, due to the occurrence of $\check{X}(t)$, the classic Lyapunov method-based stability analysis cannot be performed in a straightforward manner. However, by rearranging the correction term in the proposed STSMO, it is possible to introduce into the dynamics (11) the additive term $\boldsymbol{w}(t) = \begin{bmatrix} w_1(t) & w_2(t) \end{bmatrix}^{\text{T}} \in \mathbb{R}^2$ representinga certain class of disturbances':

$$\begin{cases} \dot{\tilde{X}}(t) = \tilde{\mu}(t)\check{X}(t) + w_1(t) \\ \qquad -2\beta\big[\overline{\rho}\big|\tilde{X}\big|\big]^{0.5}\text{sgn}\big(\check{X}(t)\big)\check{X}(t), \\ \dot{\tilde{\mu}}(t) \in U\overline{\rho}\check{X}(t) - \alpha\overline{\rho}\text{sgn}\big(\check{X}(t)\big)\check{X}(t) + w_2(t), \\ \tilde{X}(t_0) = \tilde{X}_0,\ \tilde{\mu}(t_0) = \tilde{\mu}_0. \end{cases} \tag{12}$$

Taking into account Lemma 2, the components of vector $\boldsymbol{w}(t)$ can be presented as

$$w_1(t) \triangleq rD(t)e_{\text{X}_{\text{r}}}(t) + \big[\mu(t) - m_{\text{x}} - (1+r)D(t)\big]e_{\text{X}}(t) - 2\beta\big[\overline{\rho}\big|\tilde{X}(t) - e_{\text{X}}(t)\big|\big]^{0.5}$$

$$\times \operatorname{sgn}\big(\tilde{X}(t) - e_{\mathrm{X}}(t)\big)\check{X}(t) + 2\beta\big[\overline{\rho}\big|\tilde{X}(t)\big|\big]^{0.5}\operatorname{sgn}\big(\tilde{X}(t)\big)\check{X}(t),$$

$$w_2(t) \triangleq U\overline{\rho}e_{\mathrm{X}}(t) + \alpha\overline{\rho}\check{X}(t)\big[\operatorname{sgn}\big(\tilde{X}(t)\big) - \operatorname{sgn}\big(\tilde{X}(t) - e_{\mathrm{X}}(t)\big)\big].$$

The transition from (11) to (12) can be understood in that there exists a 'nominal' observer for the system (9), i.e., comprising direct measurements of $X(t)$ and $X_{\mathrm{r}}(t)$, when its dynamics are affected by $\boldsymbol{w}(t)$. Furthermore, taking into account Lemma 2, and together with Assumptions 2, 4, and 7, it can be claimed that vector $\boldsymbol{w}(t)$ is asymptotically vanishing to zero point $\boldsymbol{w}_{\mathrm{e}} = (0,0) \in \mathbb{R}^2$ for any initial conditions. Also, this vector is uniformly bounded for every $t \in \mathbb{T}$:

$$\begin{aligned} |w_1(t)| &\leq \overline{w_1} = \max\{|w_1(t)| : t \in \mathbb{T}\}, \\ |w_2(t)| &\leq \overline{w_2} = \max\{|w_2(t)| : t \in \mathbb{T}\}, \\ \overline{w} &= ||\begin{bmatrix}\overline{w_1} & \overline{w_2}\end{bmatrix}^{\mathrm{T}}||_2 \in \mathbb{R}_+, \end{aligned} \tag{13}$$

where both $\overline{w_1}$, $\overline{w_2} \in \mathbb{R}_+$ are taken conservatively.

Let us apply the following global and homeomorphic state transformation (De Battista *et al*., 2012; Moreno and Osorio, 2012; Moreno, 2012) to the error dynamics (12):

$$\boldsymbol{\xi}(t) \triangleq \Big[\big[\overline{\rho}\big|\tilde{X}(t)\big|\big]^{0.5}\operatorname{sgn}\big(\tilde{X}(t)\big) \quad \tilde{\mu}(t)\Big]^{\mathrm{T}} \in \boldsymbol{\Xi} \subset \mathbb{R}^2. \tag{14}$$

Next, knowing that, for any $t \in \mathbb{T}$, $\operatorname{sgn}\big(\tilde{X}(t)\big) = \operatorname{sgn}(\xi_1(t))$ and $\dot{\xi}_1(t) = 0.5\overline{\rho}\,|\xi_1(t)|^{-1}\dot{\tilde{X}}(t)$, the transformation (14) converts the error dynamics (12) to the following differential inclusion:

$$\begin{cases} \dot{\boldsymbol{\xi}}(t) \in \overline{\rho}\,(|\xi_1(t)|)^{-1}\left[\check{X}(t)\boldsymbol{\Lambda}\boldsymbol{\xi}(t) + \boldsymbol{\omega}(t)\right], \\ \boldsymbol{\xi}(t_0) = \boldsymbol{\xi}_0, \end{cases} \tag{15}$$

where for every $t \in \mathbb{T}$ we have here that : $\boldsymbol{\omega}(t) \triangleq \big[0.5w_1(t) \quad |\xi_1(t)|\,(\overline{\rho})^{-1}w_2(t)\big]^{\mathrm{T}} \in \mathbb{R}^2$ is bounded by term $\overline{\omega} = \Big\|\big[\overline{\omega_1} \quad \overline{\omega_2}\big]^{\mathrm{T}}\Big\|_2 \in \mathbb{R}_+$, $\big|\xi_1(t)\big| \leq \big[\overline{\rho}\tilde{X}_{\mathrm{b}}\big]^{0.5}$ and $\boldsymbol{\Lambda} \subset \mathbb{R}^{2\times 2}$ denotes the convex polytope 'playing the role' of the state matrix (Boyd *et al*., 1994).

The differential inclusion (15) can be presented as the linear (affine) polytopic differential inclusion, i.e., the polytope $\boldsymbol{\Lambda}$ becomes equivalent to the following convex hull (De Battista *et al*., 2012; Nuñez *et al*., 2013):

$$\begin{aligned} &\forall t \in \mathbb{T}\colon \boldsymbol{\Lambda} = \operatorname{conv}\{\boldsymbol{\mathcal{A}}_1, \boldsymbol{\mathcal{A}}_2\}, \quad \boldsymbol{\mathcal{A}}_1, \boldsymbol{\mathcal{A}}_2 \in \mathbb{R}^{2\times 2} \\ &\boldsymbol{\mathcal{A}}_1 = \begin{bmatrix} -\beta & 0.5 \\ -(\alpha-1) & 0 \end{bmatrix}, \\ &\boldsymbol{\mathcal{A}}_2 = \begin{bmatrix} -\beta & 0.5 \\ -(\alpha+1) & 0 \end{bmatrix}. \end{aligned} \tag{16}$$

If the differential inclusion (15) is unperturbed and the convex hull (16) is given, then, for any time dependent matrix $\boldsymbol{\mathcal{A}}(t) \in \boldsymbol{\Lambda}\ \forall t \in \mathbb{T}$, $\boldsymbol{\mathcal{A}}\colon \mathbb{T} \to \mathbb{R}^{2\times 2}$, the quadratic global asymptotic and uniform stability of $\boldsymbol{\xi}(t)$ is ensured if $\alpha > 1$ and $\beta > 0$.

This means that for the subsequent Lyapunov equation (inequality) and quadratic Lyapunov function (analogous to (6)) $\mathcal{V}_{\mathrm{S}}(\boldsymbol{\xi}(t), t) : \boldsymbol{\Xi} \times \mathbb{T} \to \mathbb{R}_+ \cup \{0\}$ (Khalil, 2002; Moreno, 2012),

$$\begin{aligned} &\mathcal{V}_{\mathrm{S}}(\boldsymbol{\xi}(t), t) = \boldsymbol{\xi}^{\mathrm{T}}(t)\boldsymbol{\mathcal{P}}_{\mathrm{S}}\boldsymbol{\xi}(t), \\ &\underline{\lambda}(\boldsymbol{\mathcal{P}}_{\mathrm{S}})\,\|\boldsymbol{\xi}(t)\|_2^2 \leq \mathcal{V}_{\mathrm{S}}(\boldsymbol{\xi}(t), t) \leq \overline{\lambda}(\boldsymbol{\mathcal{P}}_{\mathrm{S}})\,\|\boldsymbol{\xi}(t)\|_2^2, \\ &-\underline{\lambda}(\boldsymbol{\mathcal{Q}}_{\mathrm{S}})\,\boldsymbol{I}_{2\times 2} > -\boldsymbol{\mathcal{Q}}_{\mathrm{S}} = \boldsymbol{\mathcal{A}}^{\mathrm{T}}(t)\boldsymbol{\mathcal{P}}_{\mathrm{S}} + \boldsymbol{\mathcal{P}}_{\mathrm{S}}\boldsymbol{\mathcal{A}}(t), \\ &\boldsymbol{\mathcal{P}}_{\mathrm{S}} \in \mathbb{R}_+^{2\times 2}, \quad \boldsymbol{\mathcal{Q}}_{\mathrm{S}} \in \mathbb{R}_+^{2\times 2}, \end{aligned} \tag{17}$$

there exists a feasible solution to the quasi-convex linear matrix inequality (LMI) (Boyd *et al*., 1994). Moreover, the Lyapunov matrix $\boldsymbol{\mathcal{P}}_{\mathrm{S}}$ is 'common' for any $\boldsymbol{\mathcal{A}}(t) \in \boldsymbol{\Lambda}$, and $\underline{\lambda}(\boldsymbol{\mathcal{Q}}_{\mathrm{S}}) \in \mathbb{R}_+$ denotes the smallest eigenvalue selected from among any possible spectrum of $\boldsymbol{\mathcal{Q}}_{\mathrm{S}}$ (De Battista *et al*., 2012; Nuñez *et al*., 2013). The key properties of the quadratic Lyapunov function, which is an absolutely continuous and continuously differentiable function except set $\boldsymbol{\Gamma} = \{\boldsymbol{\xi}(t) \in \boldsymbol{\Xi}\colon \xi_1(t) = 0\}$, are introduced by Moreno (2012), Moreno and Osorio (2012) as well as Moreno and Mendoza (2014). Thus, $\mathcal{V}_{\mathrm{S}}(\boldsymbol{\xi}(t), t)$ is supposed to be monotonically decreasing and converging to $\boldsymbol{\xi}_{\mathrm{e}} = (0,0) \in \boldsymbol{\Xi}$, with respect to all non-zero solutions of (15) in time $t \in \mathbb{T}$.

However, in (15) $\boldsymbol{\omega}(t)$ can be found, which causes the differential inclusion to be perturbed. In this case, the stability proof is more elaborated compared with De Battista *et al*. (2012). By combining (15) and (17), the time derivative of $\mathcal{V}_{\mathrm{S}}(\boldsymbol{\xi}(t), t)$ yields

$$\begin{aligned} \dot{\mathcal{V}}_{\mathrm{S}}(\boldsymbol{\xi}(t), t) &= p_{\mathrm{a}}\left[\boldsymbol{\xi}^{\mathrm{T}}(t)p_{\mathrm{b}}\right] \\ &\leq p_{\mathrm{a}}\big[-\underline{\lambda}(\boldsymbol{\mathcal{Q}}_{\mathrm{S}})\,\check{X}(t)\boldsymbol{\xi}^{\mathrm{T}}(t)\boldsymbol{\xi}(t), \\ &\quad + 2\boldsymbol{\xi}^{\mathrm{T}}(t)\boldsymbol{\mathcal{P}}_{\mathrm{S}}\boldsymbol{\omega}(t)\big] \end{aligned} \tag{18}$$

where

$$\begin{aligned} p_{\mathrm{a}} &= \overline{\rho}\,(|\xi_1(t)|)^{-1}, \\ p_{\mathrm{b}} &= \check{X}(t)\left(\boldsymbol{\mathcal{A}}^{\mathrm{T}}(t)\boldsymbol{\mathcal{P}}_{\mathrm{S}} + \boldsymbol{\mathcal{P}}_{\mathrm{S}}\boldsymbol{\mathcal{A}}(t)\right)\boldsymbol{\xi}(t) \\ &\quad + 2\boldsymbol{\mathcal{P}}_{\mathrm{S}}\boldsymbol{\omega}(t). \end{aligned}$$

In general, the proof can be divided into two steps. The first step covers the issue of the global ultimate and uniform boundedness (GUUB) of vector $\boldsymbol{\xi}(t)$ in time $t \geq t_0 + T_{\mathrm{reach}}$, assuming that $\boldsymbol{\omega}(t)$ is not vanishing to the zero point. Moreover, the exact formula for time T_{reach} is delivered. The second step extends the discussion by showing that the GAES property of $\boldsymbol{\xi}(t)$ can be justified in time $t \geq t_0 + T_{\mathrm{reach}}$, assuming that $\boldsymbol{\omega}(t)$ tends to the zero point.

For the first one, let us apply the input to state stability (ISS) tools (López-Caamal and Moreno, 2016; Khalil, 2002). Hence, by invoking Lemma 2, Assumption 2, and (13) as well as (17), the Lyapunov inequality (18) can be rewritten $\forall \boldsymbol{\xi}(t) \in \boldsymbol{\Xi} \setminus \{\boldsymbol{\xi}_{\mathrm{e}}\}$ in the following way:

$$\dot{\mathcal{V}}_{\mathrm{S}}\left(\boldsymbol{\xi}(t), t\right) \leq p_{\mathrm{a}} \left\|\boldsymbol{\xi}(t)\right\|_2 \left[-p_{\mathrm{c}} - p_{\mathrm{d}} + 2\overline{\lambda}\left(\boldsymbol{\mathcal{P}}_{\mathrm{S}}\right) \left\|\boldsymbol{\omega}(t)\right\|_2 \right] < 0, \tag{19}$$

where

$$p_{\mathrm{c}} = \underline{\lambda}\left(\boldsymbol{\mathcal{Q}}_{\mathrm{S}}\right) \chi \check{\underline{X}} \left\|\boldsymbol{\xi}(t)\right\|_2,$$
$$p_{\mathrm{d}} = \underline{\lambda}\left(\boldsymbol{\mathcal{Q}}_{\mathrm{S}}\right) (1-\chi) \check{\underline{X}} \left\|\boldsymbol{\xi}(t)\right\|_2,$$

$\chi \in (0\ ,\ 1) \subset \mathbb{R}_+$ and $\check{\underline{X}} \in \mathbb{R}_+$ is the lower bound of the biomass concentration-related pseudo-measurement.

It can be realised that the derivative (19) is negative if the following condition holds $\forall t \in \mathbb{T}$ (Khalil, 2002; Moreno and Osorio, 2012; Moreno, 2012):

$$\dot{\mathcal{V}}_{\mathrm{S}}\left(\boldsymbol{\xi}(t), t\right) \leq -\underline{\lambda}\left(\boldsymbol{\mathcal{Q}}_{\mathrm{S}}\right) \chi \overline{\rho} \check{\underline{X}} \left(\left|\xi_1(t)\right|\right)^{-1} \left\|\boldsymbol{\xi}(t)\right\|_2^2 < 0 \tag{20}$$

if

$$\underline{\lambda}\left(\boldsymbol{\mathcal{Q}}_{\mathrm{S}}\right) (1-\chi) \check{\underline{X}} \left\|\boldsymbol{\xi}(t)\right\|_2 \geq 2\overline{\lambda}\left(\boldsymbol{\mathcal{P}}_{\mathrm{S}}\right) \overline{\omega} \geq 2\overline{\lambda}\left(\boldsymbol{\mathcal{P}}_{\mathrm{S}}\right) \left\|\boldsymbol{\omega}(t)\right\|_2.$$

In other words, if the state trajectories $\boldsymbol{\xi}(t)$ belong to the compact and invariant set $\boldsymbol{\mathcal{S}}_{\boldsymbol{\omega}} \subset \mathbb{R}_+$,

$$\boldsymbol{\mathcal{S}}_{\boldsymbol{\omega}} = \left\{ \forall \boldsymbol{\xi}(t) \in \boldsymbol{\Xi}\colon \left\|\boldsymbol{\xi}(t)\right\|_2 \geq 2\frac{\overline{\lambda}\left(\boldsymbol{\mathcal{P}}_{\mathrm{S}}\right)}{\underline{\lambda}\left(\boldsymbol{\mathcal{Q}}_{\mathrm{S}}\right)(1-\chi)\check{\underline{X}}}\overline{\omega} \right\},$$

$$\forall t \in \mathbb{T},\ \Psi = 2\frac{\overline{\lambda}\left(\boldsymbol{\mathcal{P}}_{\mathrm{S}}\right)}{\underline{\lambda}\left(\boldsymbol{\mathcal{Q}}_{\mathrm{S}}\right)(1-\chi)\check{\underline{X}}} \times \sqrt{\overline{\lambda}\left(\boldsymbol{\mathcal{P}}_{\mathrm{S}}\right)\underline{\lambda}^{-1}\left(\boldsymbol{\mathcal{P}}_{\mathrm{S}}\right)\overline{\omega}},$$

then $\dot{\mathcal{V}}_{\mathrm{S}}\left(\boldsymbol{\xi}(t), t\right)$ is locally negative definite for this set and the ultimate bound $\Psi \in \mathbb{R}_+$ is given.

Therefore, the GUUB property of $\boldsymbol{\xi}(t)$ in the finite time $t \geq t_0 + T_{\mathrm{reach}}$ is confirmed, which justifies the robustness of the estimation process of the pair $(X(t), \mu(t))$ for the case of the non-vanishing $\boldsymbol{\omega}(t)$. Next, by applying the comparison principle (Khalil, 2002; Moreno and Osorio, 2012; Moreno, 2012) with (16) and (20), the exact formula for T_{reach} is $\forall t \in \mathbb{T}$ given as

$$T_{\mathrm{reach}} \approx 2\frac{\left[\overline{\lambda}\left(\boldsymbol{\mathcal{P}}_{\mathrm{S}}\right)\right]^{1.5}}{\underline{\lambda}\left(\boldsymbol{\mathcal{Q}}_{\mathrm{S}}\right)\chi\overline{\rho}\check{\underline{X}}\sqrt{\underline{\lambda}\left(\boldsymbol{\mathcal{P}}_{\mathrm{S}}\right)}} \times \left\|\boldsymbol{\xi}(t_0)\right\|_2 \tag{21}$$

whenever

$$\left\|\boldsymbol{\xi}(t)\right\|_2 \leq \left\|\boldsymbol{\xi}(t_0)\right\|_2 \left[\frac{\overline{\lambda}\left(\boldsymbol{\mathcal{P}}_{\mathrm{S}}\right)}{\underline{\lambda}\left(\boldsymbol{\mathcal{P}}_{\mathrm{S}}\right)}\right]^{0.5} - \frac{\underline{\lambda}\left(\boldsymbol{\mathcal{Q}}_{\mathrm{S}}\right)\chi\overline{\rho}\check{\underline{X}}}{2\overline{\lambda}\left(\boldsymbol{\mathcal{P}}_{\mathrm{S}}\right)}t.$$

This property can be commented on as follows. By invoking the general idea of the AO, the asymptotic (exponential) convergence of the estimation error is only dependent on the behaviour of $\boldsymbol{u}(t)$. Knowing that the operation of the AO (4) is not anticipated as having a finite time (see Section 3.1), it is not possible to state that the AO dynamics will be faster than those of the STSMO. Therefore, for both pairs of measurements/pseud-measurements delivered to the proposed STSMO, it is clear that the tunable time T_{reach} is primarily related to them and not to the original $X(t)$ and $X_{\mathrm{r}}(t)$ generated by the system considered. Hence, it can be stated that the estimation error between pairs $(X(t), \mu(t))$ and $\left(\hat{X}(t), \hat{\mu}(t)\right)$ is globally ultimately uniformly bounded after time $t > t_0 + T_{\mathrm{reach}}$.

For the second step, the GAES property of $\boldsymbol{\xi}(t)$ is justified when $\boldsymbol{\omega}(t)$ vanishes asymptotically (see Lemma 2). Taking into account the existence of the time instant T_{reach} (21), there is a constant $\overline{\omega}_{\mathrm{T}} = \left\|\boldsymbol{\omega}(T_{\mathrm{reach}})\right\|_2 \in \mathbb{R}_+$, $\overline{\omega}_{\mathrm{T}} < \overline{\omega}$ preserving its GUUB property. Therefore, the bounded set $\boldsymbol{\mathcal{S}}_{\boldsymbol{\omega}} \subset \boldsymbol{\mathcal{S}}_{\mathrm{R}} \subset \boldsymbol{\Xi}$ is given as follows: for every $t \in \mathbb{T}$,

$$\boldsymbol{\mathcal{S}}_{\mathrm{R}} = \left\{ \forall \boldsymbol{\xi}(t) \in \boldsymbol{\Xi}\colon \left\|\boldsymbol{\xi}(t)\right\|_2 \geq 2\frac{\overline{\lambda}\left(\boldsymbol{\mathcal{P}}_{\mathrm{S}}\right)}{\underline{\lambda}\left(\boldsymbol{\mathcal{Q}}_{\mathrm{S}}\right)(1-\chi)\check{\underline{X}}}\overline{\omega}_{\mathrm{T}} \right\}.$$

Now, it can be noticed that the relationship between $\boldsymbol{\xi}(t)$ and $\boldsymbol{\omega}(t)$ from (20) imposes the following property. If $\left\|\boldsymbol{\omega}(t)\right\|_2$ tends to zero asymptotically for any initial conditions, then $\left\|\boldsymbol{\xi}(t)\right\|_2 \to 0$ as $t \to \infty$. This coincides simultaneously with the fact that the derivative of the Lyapunov function is globally negative semi-definite in the whole set $\boldsymbol{\Xi}$, i.e., $\dot{\mathcal{V}}_{\mathrm{S}}\left(\boldsymbol{\xi}(t), t\right) = 0$ only at the equilibrium point $\boldsymbol{\xi}_{\mathrm{e}}$. This particular property can be explained by applying the theory of limit sets (Khalil, 2002). Assume that there exists a sequence of time moments $\{t\}_{\vartheta}^{\infty} \subset \mathbb{T}$, $\vartheta \in \mathbb{N}_+$, where $t_1 = T_{\mathrm{reach}}$, and $t_\vartheta \to \infty$, as well as $\vartheta \to \infty$. Then, by taking $\boldsymbol{\xi}\left(t_\vartheta\right) \equiv \boldsymbol{\xi}_\vartheta$, $\boldsymbol{\mathcal{S}}_{\mathrm{R}} \equiv \boldsymbol{\mathcal{S}}_1$ and $\boldsymbol{\xi}(t_1) \equiv \boldsymbol{\xi}\left(T_{\mathrm{reach}}\right)$, the following dependence holds: if

$$0 \leq \left\|\boldsymbol{\omega}\left(t_{\vartheta+1}\right)\right\|_2 < \left\|\boldsymbol{\omega}\left(t_\vartheta\right)\right\|_2,$$

then

$$\boldsymbol{\mathcal{S}}_\vartheta \subset \boldsymbol{\mathcal{S}}_{\vartheta+1} \subset \mathbb{R}_+ \cup \{0\}, \quad \forall \vartheta \in \mathbb{N}_+.$$

As a result, if (20) holds, then for all consecutive $t_\vartheta \in \mathbb{T}$ the distance function $\operatorname{dist}(\boldsymbol{\xi}_\mathrm{e}, \boldsymbol{\mathcal{S}}_\vartheta)$ and the Lyapunov function $\mathcal{V}_\mathrm{S}(t_\vartheta)$ satisfy

$$\operatorname{dist}(\boldsymbol{\xi}_\mathrm{e}, \boldsymbol{\mathcal{S}}_\vartheta) = \inf\Big\{ \|\boldsymbol{\xi}_\vartheta\|_2 \in \boldsymbol{\mathcal{S}}_\vartheta : \big| \|\boldsymbol{\xi}_\vartheta\|_2 - \|\boldsymbol{\xi}_\mathrm{e}\|_2 \big| \Big\} \to 0,$$

and

$$0 \leq \mathcal{V}_\mathrm{S}(\boldsymbol{\xi}_{\vartheta+1}, t_{\vartheta+1}) < \mathcal{V}_\mathrm{S}(\boldsymbol{\xi}_\vartheta, t_\vartheta), \quad \forall \vartheta \in \mathbb{N}_+.$$

Thus, the family of sets $\boldsymbol{\mathcal{S}}_\vartheta$ constitutes the sequence whose limit set $\boldsymbol{\mathcal{S}}_\mathrm{e} \in \mathbb{R}_+ \cup \{0\}$ (last element) fulfils: $\boldsymbol{\mathcal{S}}_\mathrm{e} \cap \{\|\boldsymbol{\xi}_\mathrm{e}\|_2\} \neq \emptyset$ as $\vartheta \to \infty$. To sum up, the equilibrium point $\boldsymbol{\xi}_\mathrm{e}$ is the limit point of sequence $\boldsymbol{\xi}(t_\vartheta)$ and sequence $\mathcal{V}_\mathrm{S}(t_\vartheta)$ converging to zero, fulfilling the Lyapunov theorem. Therefore, it is shown that vector $\boldsymbol{\xi}(t)$, and the pair $\big(\tilde{X}(t), \tilde{\mu}(t)\big)$ are GAES in time $t \geq t_0 + T_\mathrm{reach}$, which completes the proof. ■

Remark 4. The choice between the two above-named pairs of measurements/pseudo-measurements can significantly affect the convergence rate of $\hat{\mu}(t)$ to its real value. If $X(t)$ is directly measured and the concentration of $X_\mathrm{r}(t)$ constitutes a pseudo-measurement, then assuming the same initial conditions $\boldsymbol{x}_0$, $\hat{\boldsymbol{c}}_0$, $\hat{X}_0$, $\hat{\mu}_0$, the same values of parameters α, β, $\overline{\rho}$, and identical inputs $\boldsymbol{u}(t)$ $\forall t \in \mathbb{T}$, the convergence rate of the estimates generated by the proposed STSMO is naturally faster than when both signals are reconstructed by the proposed AO.

Proposition 3. *To avoid the chattering phenomenon, the following smooth approximations of functions* $\operatorname{sgn}(\cdot)$ *and* $|(\cdot)|$ *are proposed (Czyżniewski et al., 2023):*

$$\operatorname{sgn}(\cdot) \simeq \chi(\cdot) = \frac{(\cdot)}{\theta_1 + |(\cdot)|},$$

$$|(\cdot)| \simeq \psi(\cdot) = \theta_2^{-1}\big[\log(1 + \exp(\theta_2(\cdot))) + \log(1 + \exp(-\theta_2(\cdot)))\big],$$

where $\theta_1, \theta_2 \in \mathbb{R}_+$ *denote the tuning parameters.*

4. Case study

In order to validate the ability to reconstruct the unmeasured state variables in the presence of the uncertainty introduced by the unknown kinetic function, and to estimate this unknown kinetic function by the developed hierarchical observer, a system consisting of a bioreactor with a settler is used. This system is shown in Fig. 2.

The model of the system presented in Fig. 2 considering the microbial growth reaction and microbial mortality belonging to the class of CSTR models of the form (2) is given as follows (Dochain and Vanrolleghem, 2001; Bastin and Dochain, 1990; Hadj-Sadok and Gouzé, 2005):

$$\Sigma_\mathrm{CSTR}: \begin{cases} \dot{X}(t) = \mu(t)X(t) + rX_\mathrm{r}(t)D(t) \\ \qquad -m_\mathrm{x}X(t) - (1+r)X(t)D(t), \\ \dot{S}(t) = -\dfrac{1}{Y_\mathrm{s}}\mu(t)X(t) - m_\mathrm{s}X(t) \\ \qquad +S_\mathrm{in}(t)D(t) - (1+r)S(t)D(t), \\ \dot{DO}(t) = -\dfrac{1}{Y_\mathrm{o}}\mu(t)X(t) - m_\mathrm{o}X(t) \\ \qquad +DO_\mathrm{in}(t)D(t) \\ \qquad -(1+r)DO(t)D(t) \\ \qquad +k_\mathrm{L}a(t)(DO_\mathrm{sat} - DO(t)), \\ \dot{X}_\mathrm{r}(t) = v(1+r)X(t)D(t) \\ \qquad -v(w+r)X_r(t)D(t), \\ X(t_0) = X_0, \quad S(t_0) = S_0, \\ DO(t_0) = DO_0, \quad X_\mathrm{r}(t_0) = X_{\mathrm{r}_0}. \end{cases} \tag{22}$$

By invoking the model (1), the concentrations of two non-biomass compounds can be distinguished in the model (22). These are the concentrations of the aggregated substrate $S(t)$ $[\mathrm{mg/L}] \in \mathbb{R}_+$ and dissolved oxygen $DO(t)$ $[\mathrm{mg/L}] \in \mathbb{R}_+$. Hence, the parameters Y_s $[-] \in \mathbb{R}_+$, Y_o $[-] \in \mathbb{R}_+$ and m_s $[\mathrm{h}^{-1}] \in \mathrm{R}_+$, m_o $[\mathrm{h}^{-1}] \in \mathrm{R}_+$ are the appropriate yield and maintenance coefficients, whereas $S_\mathrm{in}(t)$ $[\mathrm{mg/L}] \in \mathbb{R}_+$, $DO_\mathrm{in}(t)$ $[\mathrm{mg/L}] \in \mathbb{R}_+$ and DO_sat $[\mathrm{mg/L}] \in \mathbb{R}_+$ stand for the concentrations of substrate, dissolved oxygen, and dissolved oxygen saturation in the inflow to the bioreactor, respectively. The gas-liquid transfer function $k_\mathrm{L}a(t)$ (see Assumption 5) is linked with the mass transfer of the dissolved oxygen concentration into the bioreactor (Lindberg, 1997; Garcia-Ochoa and Gomez, 2009; Czyżniewski *et al.*, 2023).

Proposition 4. *A large number of kinetic function models that differ in the number of variables and/or in the structure representing the biochemical processes taking place in the bioreactor can be found in the literature (Bastin and Dochain, 1990; Dewasme et al., 2013; López-Caamal and Moreno, 2016; Dochain and Vanrolleghem, 2001; Czyżniewski and Łangowski 2022b; 2022a; Hadj-Sadok and Gouzé, 2005). For the sake of developing the so-called 'virtual model' (simulator), the kinetic function fulfilling Assumption 7 is proposed to be the following product of two distinct Monod functions:*

$$\mu(t) = \mu_\mathrm{max}(t)\frac{S(t)}{K_\mathrm{s}(t) + S(t)}\frac{DO(t)}{K_\mathrm{o}(t) + DO(t)},$$

where $\forall t \in \mathbb{T}$: $\mu_\mathrm{max}(t)$ $[\mathrm{h}^{-1}] \in \mathbb{R}_+$, $K_\mathrm{s}(t)$ $[\mathrm{mg/L}] \in \mathbb{R}_+$, *and* $K_\mathrm{o}(t)$ $[\mathrm{mg/L}] \in \mathbb{R}_+$ *denote the bounded time-varying coefficients of the maximum specific growth rate,*

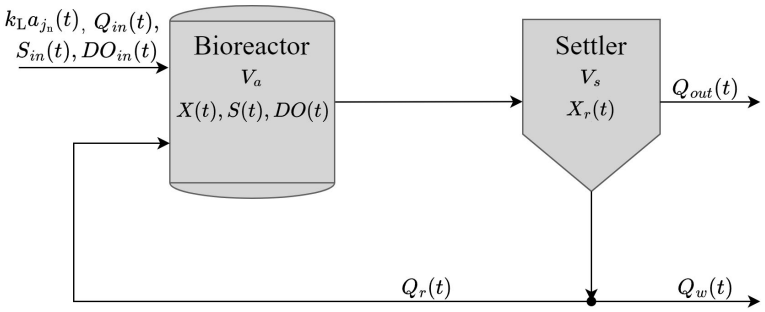

Fig. 2. Diagram of the system considered.

Table 1. Ranges and values of signals and parameters.

No.	Symbol	Value/Range	Unit
1.	$D(t)$	$[0.155,\ 0.325]$	$[\mathrm{h}^{-1}]$
2.	$k_{\mathrm{L}}a(t)$	$[11.755,\ 26.239]$	$[\mathrm{h}^{-1}]$
3.	DO_{in}	100	$[\mathrm{mg/L}]$
4.	DO_{sat}	30	$[\mathrm{mg/L}]$
5.	K_{o}	$[3.5,\ 6.5]$	$[\mathrm{mg/L}]$
6.	K_{s}	$[17.5,\ 32.5]$	$[\mathrm{mg/L}]$
7.	m_{o}	0.01	$[\mathrm{h}^{-1}]$
8.	m_{s}	0.02	$[\mathrm{h}^{-1}]$
9.	m_{x}	0.05	$[\mathrm{h}^{-1}]$
10.	S_{in}	150	$[\mathrm{mg/L}]$
11.	r	1	$[-]$
12.	v	2	$[-]$
13.	w	0.05	$[-]$
14.	$\mu_{\max}$	$[0.28,\ 0.54]$	$[\mathrm{h}^{-1}]$
15.	Y_{o}	1.8	$[-]$
16.	Y_{s}	0.8	$[-]$

saturation of substrate concentration, and saturation of dissolved oxygen concentration, respectively.

To impose the presentation-related coherency, the vectors of state variables and inputs of the CSTR model (see Assumptions 1 and 4) are defined as

$$\begin{aligned}\boldsymbol{x}(t) &\triangleq \begin{bmatrix}x_1(t) & x_2(t) & x_3(t) & x_4(t)\end{bmatrix}^{\mathrm{T}}\\ &= \begin{bmatrix}X(t) & S(t) & DO(t) & X_{\mathrm{r}}(t)\end{bmatrix}^{\mathrm{T}},\\ \boldsymbol{u}(t) &\triangleq \begin{bmatrix}u_1(t) & u_2(t) & u_3(t) & u_4(t)\end{bmatrix}^{\mathrm{T}}\\ &= \begin{bmatrix}D(t) & D(t)S_{\mathrm{in}}(t) & D(t)DO_{\mathrm{in}}(t) & k_{\mathrm{L}}a(t)\end{bmatrix}^{\mathrm{T}}.\end{aligned} \tag{23}$$

The ranges and values of particular signals and parameters are outlined in Table 1. As can be noticed, the values of parameters related to the kinetic function (see Proposition 4) are burdened by parametric uncertainty.

4.1. Hierarchical observer design. This section presents the synthesis of the hierarchical observer for the model (22) for different measured outputs (see Assumption 3). More specifically, cases are considered where the measured output is the concentration of aggregated biomass, i.e., $y(t) = h(\boldsymbol{x}(t)) = X(t)$, or the concentration of aggregated substrate, i.e., $y(t) = h(\boldsymbol{x}(t)) = S(t)$.

4.1.1. AO design with aggregated biomass concentration measurement. According to Section 3.1 and by defining the measured output as $y(t) \triangleq X(t)$, we get

$$c_1(t) \triangleq S(t), \quad c_2(t) \triangleq DO(t), \quad c_3(t) \triangleq X_{\mathrm{r}}(t),$$

$$\mathbf{1}_{(\mathrm{n}-1\times 1)} \triangleq \begin{bmatrix}1\\1\\0\end{bmatrix}, \quad \boldsymbol{F} \triangleq \begin{bmatrix}Y_{\mathrm{s}} & 0 & 0\\ 0 & Y_{\mathrm{o}} & 0\\ 0 & 0 & 1\end{bmatrix}. \tag{24}$$

By combining (22) and (24), the following AO structure is obtained:

$$\Sigma^{\mathrm{X}}_{\mathrm{AO}}\colon \begin{cases}\dot{\hat{\boldsymbol{c}}}(t) = \boldsymbol{A}(\boldsymbol{u}(t))\hat{\boldsymbol{c}}(t) + \boldsymbol{B}(y(t), \boldsymbol{u}(t)),\\ \hat{\boldsymbol{v}}(t) = \boldsymbol{F}^{-1}\left[\hat{\boldsymbol{c}}(t) - \mathbf{1}_{(\mathrm{n}-1\times 1)}y(t)\right],\\ \hat{\boldsymbol{c}}(t_0) = \hat{\boldsymbol{c}}_0\end{cases} \tag{25}$$

where

$$\begin{aligned}&\boldsymbol{A}(\boldsymbol{u}(t))\\ &= \begin{bmatrix}-(1+r)u_1(t) & 0 & ru_1(t)\\ 0 & -(1+r)u_1(t) - u_4(t) & ru_1(t)\\ 0 & 0 & A\end{bmatrix},\end{aligned}$$

$$A = -v(w+r)u_1(t),$$

$$\begin{aligned}&\boldsymbol{B}(y(t), \boldsymbol{u}(t))\\ &= \begin{bmatrix}Y_{\mathrm{s}}u_2(t) - (m_{\mathrm{x}} + Y_{\mathrm{s}}m_{\mathrm{s}})y(t)\\ Y_{\mathrm{o}}u_3(t) - (m_{\mathrm{x}} + Y_{\mathrm{o}}m_{\mathrm{o}})y(t) + u_2(t)y(t) + B\\ v(1+r)u_1(t)y(t)\end{bmatrix},\end{aligned}$$

$$B = Y_{\mathrm{o}}DO_{\mathrm{sat}}u_4(t).$$

According to the conditions introduced in the proof of Theorem 1, the following eigenvalues $\lambda^{\mathrm{X}}_{i_{\mathrm{x}}}[\boldsymbol{A}(\boldsymbol{u}(t))] \in$

$\mathbb{C},\ i_{\mathrm{x}} = \overline{1,3}$ of matrix $\boldsymbol{A}(\boldsymbol{u}(t))$ defined in (25) are given $\forall t \in \mathbb{T}$:

$$\begin{aligned}
\lambda_1^{\mathrm{X}}\left[\boldsymbol{A}(\boldsymbol{u}(t))\right] &= -2u_1(t) - u_4(t) \leq -12.065,\\
\lambda_2^{\mathrm{X}}\left[\boldsymbol{A}(\boldsymbol{u}(t))\right] &= -2u_1(t) \leq -0.31,\\
\lambda_3^{\mathrm{X}}\left[\boldsymbol{A}(\boldsymbol{u}(t))\right] &= -2.1u_1(t) \leq -0.3255.
\end{aligned}$$

Due to the fact that for every $t \in \mathbb{T}$ all inputs $\boldsymbol{u}(t)$ are positive and uniformly bounded (see Assumption 4), the internal dynamics of the designed AO (25) are globally asymptotically stable.

4.1.2. AO design with aggregated substrate concentration measurement. According to Section 3.1 and by defining the measured output as $y(t) \triangleq S(t)$, we get

$$c_1(t) \triangleq X(t), \quad c_2(t) \triangleq DO(t), \quad c_3(t) \triangleq X_{\mathrm{r}}(t),$$

$$\boldsymbol{K} \triangleq \begin{bmatrix} Y_{\mathrm{s}} & -Y_{\mathrm{s}}/Y_{\mathrm{o}} & 0 \end{bmatrix}^{\mathrm{T}}. \tag{26}$$

By combining (22) with (26), the following AO structure is obtained:

$$\Sigma_{\mathrm{AO}}^{\mathrm{S}}\colon \begin{cases} \dot{\hat{\boldsymbol{c}}}(t) = \boldsymbol{A}(\boldsymbol{u}(t))\hat{\boldsymbol{c}}(t) + \boldsymbol{B}(y(t), \boldsymbol{u}(t)),\\ \hat{\boldsymbol{v}}(t) = \hat{\boldsymbol{c}}(t) - \boldsymbol{K}y(t),\\ \hat{\boldsymbol{c}}(t_0) = \hat{\boldsymbol{c}}_0 \end{cases} \tag{27}$$

where

$$\begin{aligned}
&\boldsymbol{A}(\boldsymbol{u}(t))\\
&= \begin{bmatrix} A_1 & 0 & ru_1(t)\\ A_2 & -(1+r)u_1(t) - u_4(t) & 0\\ A_3 & 0 & -v(w+r)u_1(t) \end{bmatrix},
\end{aligned}$$

$$\boldsymbol{B}(y(t), \boldsymbol{u}(t)) = \begin{bmatrix} B_1\\ B_2\\ -Y_{\mathrm{s}}v(1+r)u_1(t)y(t) \end{bmatrix}$$

and

$$\begin{aligned}
A_1 &= -m_{\mathrm{x}} - Y_{\mathrm{s}}m_{\mathrm{s}} - (1+r)u_1(t),\\
A_2 &= Y_{\mathrm{s}}m_{\mathrm{s}}/Y_{\mathrm{o}} - m_{\mathrm{o}},\\
A_3 &= v(r+1)u_1(t),
\end{aligned}$$

$$\begin{aligned}
B_1 &= Y_{\mathrm{s}}(m_{\mathrm{x}} + (1+r)u_1(t) + Y_{\mathrm{s}}m_{\mathrm{s}})y(t)\\
&\quad + Y_{\mathrm{s}}u_2(t) - Y_{\mathrm{s}}(1+r)u_1(t)y(t),\\
B_2 &= u_3(t) + (Y_{\mathrm{s}}/Y_{\mathrm{o}})(1+r)u_1(t)y(t)\\
&\quad - (Y_{\mathrm{s}}/Y_{\mathrm{o}})u_2(t) + DO_{\mathrm{sat}}u_2(t)\\
&\quad + m_{\mathrm{o}}Y_{\mathrm{s}}y(t) + (Y_{\mathrm{s}}/Y_{\mathrm{o}})y(t)(u_1(t) - u_4(t))\\
&\quad - (Y_{\mathrm{s}}^2/Y_{\mathrm{o}})m_{\mathrm{s}}y(t).
\end{aligned}$$

According to the conditions introduced in the proof of Theorem 1, the following eigenvalues $\lambda_{i_{\mathrm{x}}}^{\mathrm{S}}\left[\boldsymbol{A}(\boldsymbol{u}(t))\right] \in \mathbb{C},\ i_{\mathrm{S}} = \overline{1,3}$ of matrix $\boldsymbol{A}(\boldsymbol{u}(t))$ defined in (27) are given $\forall t \in \mathbb{T}$:

$$\begin{aligned}
\lambda_1^{\mathrm{S}}\left[\boldsymbol{A}(\boldsymbol{u}(t))\right] &= -2u_1(t) - u_4(t) \leq -12.065,\\
\lambda_2^{\mathrm{S}}\left[\boldsymbol{A}(\boldsymbol{u}(t))\right] &= -2.05u_1(t) - 0.033 - 0.001\Upsilon(u_1(t))\\
&\leq -0.3509,\\
\lambda_3^{\mathrm{S}}\left[\boldsymbol{A}(\boldsymbol{u}(t))\right] &= -2.05u_1(t) - 0.033 + 0.001\Upsilon(u_1(t))\\
&\leq -0.3504,\\
\Upsilon(u_1(t)) &= \sqrt{4002500u_1^2(t) - 3300u_1(t) + 1089}.
\end{aligned}$$

Due to the fact that for every $t \in \mathbb{T}$ all inputs $\boldsymbol{u}(t)$ are positive and uniformly bounded (see Assumption 4), the expressions $\Upsilon(u_1(t)) \in \mathbb{R}_+,\ \forall u_1(t) \in \mathbb{U}_{\mathrm{p}}$ are uniformly bounded, i.e., $\Upsilon(u_1(t)) \in [0.155\,;\,0.325]$. Thus, the internal dynamics of the designed AO (27) is globally asymptotically stable.

4.1.3. STSMO design with aggregated biomass concentration measurement. Taking the measured output as $y(t) \triangleq X(t)$, the structure of the STSMO comes directly from (10), and only $\widehat{X}_{\mathrm{r}}(t)$ constitutes the pseudo-measurement provided by the AO designed in Section 4.1.1. Hence, the designed STSMO is given as

$$\Sigma_{\mathrm{STSMO}}^{\mathrm{X}}\colon \begin{cases} \dot{\hat{X}}(t) = \left(\hat{\mu}(t) - m_{\mathrm{x}} - (1+r)D(t)\right)X(t)\\ \qquad\quad +r\widehat{X}_{\mathrm{r}}(t)D(t)\\ \qquad\quad +2\beta\left[\overline{\rho}\middle|X(t) - \hat{X}(t)\middle|\right]^{0.5}\\ \qquad\quad \times\mathrm{sgn}\big(X(t) - \hat{X}(t)\big)X(t),\\ \dot{\hat{\mu}}(t) = \big(\alpha\overline{\rho}\mathrm{sgn}\big(X(t) - \hat{X}(t)\big)\big)X(t),\\ \hat{X}(t_0) = \hat{X}_0,\ \hat{\mu}(t_0) = \mu_0. \end{cases} \tag{28}$$

The selection of tuning parameters α, β and $\overline{\rho}$ is explained in the next section, where the simulation study is presented.

4.1.4. STSMO design with aggregated substrate concentration measurement. Taking the measured output as $y(t) \triangleq S(t)$, the structure of the STSMO comes directly from (10) but both biomass concentrations, i.e., $\widehat{X}(t)$ and $\widehat{X}_{\mathrm{r}}(t)$, constitute the pseudo-measurements provided by the AO designed in Section 4.1.2. Hence, the designed STSMO is given as

$$\Sigma_{\mathrm{STSMO}}^{\mathrm{S}}\colon \begin{cases} \dot{\hat{X}}(t) = \left(\hat{\mu}(t) - m_{\mathrm{x}} - (1+r)D(t)\right)\widehat{X}(t)\\ \qquad\quad +r\widehat{X}_{\mathrm{r}}(t)D(t)\\ \qquad\quad +2\beta\left[\overline{\rho}\middle|\widehat{X}(t) - \hat{X}(t)\middle|\right]^{0.5}\\ \qquad\quad \times\mathrm{sgn}\big(\widehat{X}(t) - \hat{X}(t)\big)\widehat{X}(t),\\ \dot{\hat{\mu}}(t) = \big(\alpha\overline{\rho}\mathrm{sgn}\big(\widehat{X}(t) - \hat{X}(t)\big)\big)\widehat{X}(t),\\ \hat{X}(t_0) = \hat{X}_0,\ \hat{\mu}(t_0) = \mu_0. \end{cases} \tag{29}$$

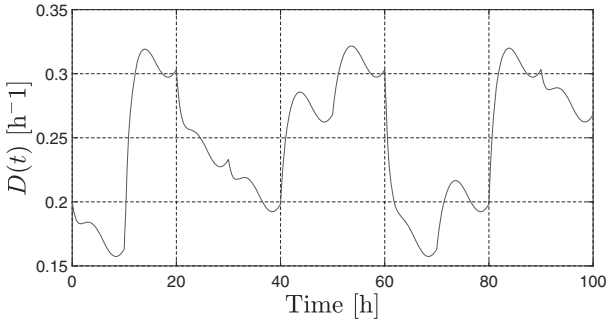

Fig. 3. Trajectory of dilution rate $D(t)$.

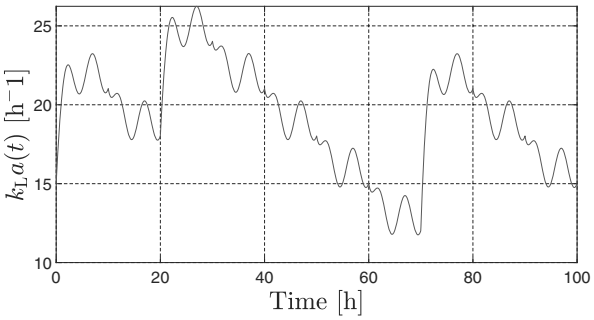

Fig. 4. Trajectory of gas-liquid transfer function $k_{\mathrm{L}}a(t)$.

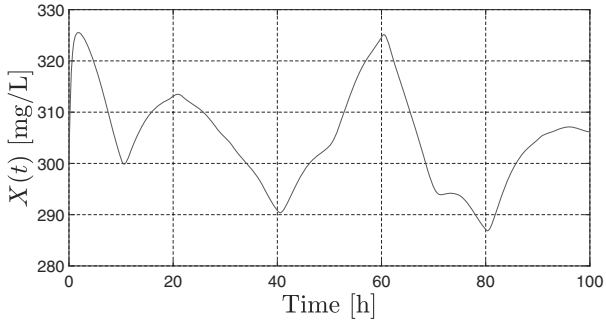

Fig. 5. Aggregated biomass concentration $X(t)$ measurement trajectory.

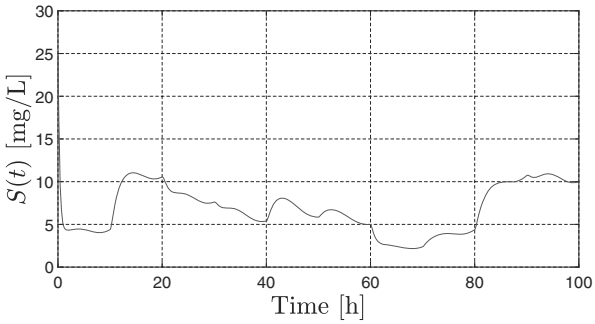

Fig. 6. Aggregated substrate concentration $S(t)$ measurement trajectory.

The selection of tuning parameters α, β and $\overline{p}$ is explained in the next section, where the simulation study is presented.

4.2. Simulation results. The devised hierarchical observers (25) and (28), as well as (27) and (29) have been applied to the CSTR model (22). This model and all observers was implemented in the Matlab/Simulink environment.

The adopted input ranges, i.e., $D(t)$ and $k_{\mathrm{L}}a(t)$, set in Table 1, represent the boundary values of their trajectories shown in Figs. 3 and 4, respectively. In turn, the variability (shape) of these trajectories within the adopted ranges was established based on other trajectories of these variables available in the literature. Various literature items were used to establish the values contained in Table 1. On the other hand, the trajectories of the measured outputs, i.e., the measurably available state variables, $X(t)$ and $S(t)$, presented in Figs. 5 and 6, were generated by employing the model (22).

It should be noted that the dynamics of the modelled system allows the measurement noise to be neglected. This situation is often found in the literature when using biomass or substrate concentration measurements. This assumption should be modified so that the dissolved oxygen concentration is used as a measurement. Then, the use of the developed hierarchical observer has to be completed with the appropriate treatment of the dissolved oxygen concentration measurement to consider the dynamics of the measuring device and filter out the measurement noise. One possible solution to this problem can be found in the work of Czyżniewski *et al*. (2023).

The simulation time was assumed as 150 [h], although some results were presented on a shorter time scale. This was due to the fact that the repeatability of the trajectories of inputs and measurements after 100 [h] was used. Thus, wherever the estimation results unambiguously showed the convergence of the estimation trajectories to the originals on the shorter time scale, the simulation calculation was not extended to 150 [h].

Taking the above into account, a series of simulation experiments for the two measurement scenarios were carried out, the selected results of which are shown in the next sections. These results are presented with the following initial conditions for the model (22): $\boldsymbol{x}_0 = \begin{bmatrix}300 & 25 & 35 & 700\end{bmatrix}^{\mathrm{T}}$. In turn, to test the performance of the developed hierarchical observer, the following three sets of initial conditions, different for a given measured output, were assumed for the unmeasured state variables.

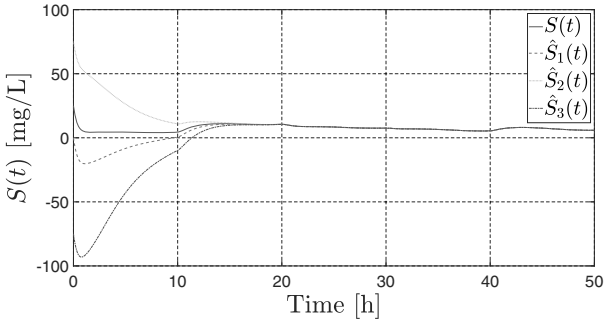

Fig. 7. Trajectories of $S(t)$ and its estimates $\hat{S}(t)$ for measurement $X(t)$.

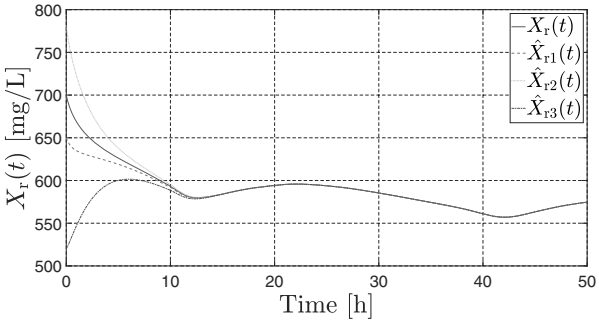

Fig. 9. Trajectories of $X_{\mathrm{r}}(t)$ and its estimates $\hat{X}_{\mathrm{r}}(t)$ for measurement $X(t)$.

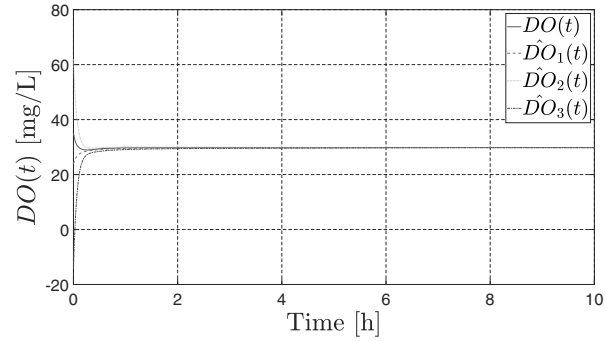

Fig. 8. Trajectories of $DO(t)$ and its estimates $\hat{DO}(t)$ for measurement $X(t)$.

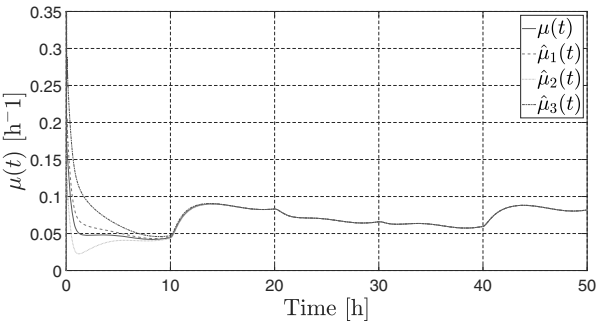

Fig. 10. Trajectories of $\mu(t)$ and its estimates $\hat{\mu}(t)$ for measurement $X(t)$.

In detail, for the measured output $X(t)$,

$$\hat{\boldsymbol{c}}_1(t_0) = \begin{bmatrix}360 & 411 & 780\end{bmatrix}^{\mathrm{T}},$$
$$\hat{\boldsymbol{c}}_2(t_0) = \begin{bmatrix}240 & 274 & 520\end{bmatrix}^{\mathrm{T}},$$
$$\hat{\boldsymbol{c}}_3(t_0) = \begin{bmatrix}420 & 480 & 910\end{bmatrix}^{\mathrm{T}},$$

while for $S(t)$

$$\hat{\boldsymbol{c}}_1(t_0) = \begin{bmatrix}330 & 31.8 & 715\end{bmatrix}^{\mathrm{T}},$$
$$\hat{\boldsymbol{c}}_2(t_0) = \begin{bmatrix}270 & 26 & 585\end{bmatrix}^{\mathrm{T}},$$
$$\hat{\boldsymbol{c}}_3(t_0) = \begin{bmatrix}360 & 37 & 780\end{bmatrix}^{\mathrm{T}}.$$

Knowing that the convergence of the designed AO is always dependent on the behaviour of vector $\boldsymbol{u}(t)$, it was necessary to select the values of the tuning parameters for the designed STSMO. For all the results presented, they were $\alpha = 2$, $\beta = 1.5$, $\overline{p} = 0.1$. In turn, the parameter values of the approximating functions (see Proposition 3) were $\theta_1 = 0.01$ and $\theta_2 = 0.001$.

4.2.1. Estimation results: Aggregated biomass concentration measurement. In this section, the estimation results obtained using the hierarchical observers (25) and (28) are presented. The trajectories of state variables representing $S(t)$, $DO(t)$, and $X_{\mathrm{r}}(t)$, and the kinetic function $\mu(t)$ which were generated by the model (22) and their estimates from the AO (25) and the STSMO (28) are shown in Figs. 7, 8, 9 and 10, respectively.

Analysing the trajectories presented in Figs. 7–9, it can be concluded that the estimation performance for the state variable representing the concentration of dissolved oxygen is very high practically from the beginning of the simulation, while for the other two state variables this performance is satisfactory after about 13 [h]. This difference in the rate of convergence is due to different time scales in the dynamics of particular state variables. Naturally, it also results from the design of the developed hierarchical observer, which takes into account the variability and value of the measurably available state variable (measured output) and the vector of inputs. In turn, the behaviour of the original and reconstructed kinetic function (see Fig. 10) shows that the tracking of the unknown kinetic function using the sliding term of the developed observer is satisfactory. Moreover, the estimate $\mu(t)$ converges to its real trajectory at the rate of convergence of the unmeasured state variables.

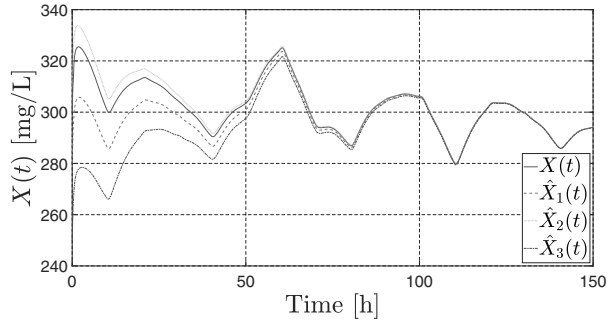

Fig. 11. Trajectories of $X(t)$ and its estimates $\hat{X}(t)$ for measurement $S(t)$.

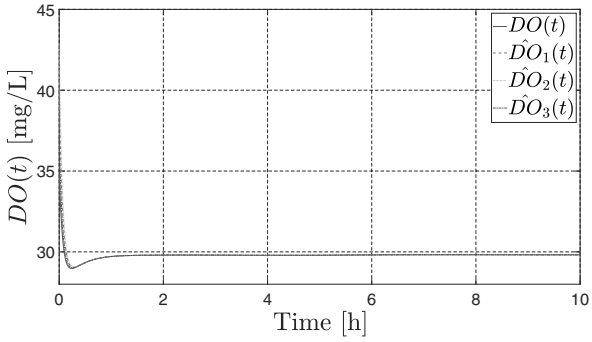

Fig. 12. Trajectories of $DO(t)$ and its estimates $\hat{DO}(t)$ for measurement $S(t)$.

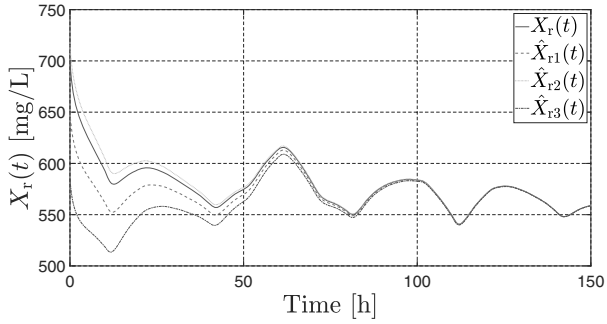

Fig. 13. Trajectories of $X_\mathrm{r}(t)$ and its estimates $\hat{X}_\mathrm{r}(t)$ for measurement $S(t)$.

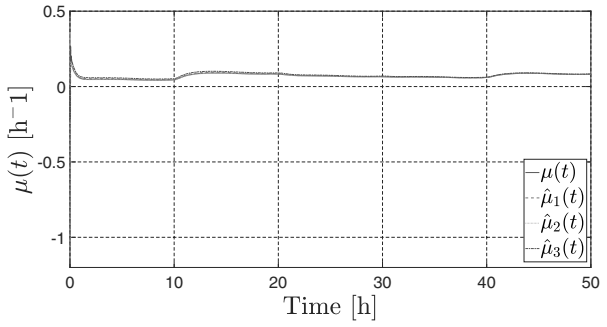

Fig. 14. Trajectories of $\mu(t)$ and its estimates $\hat{\mu}(t)$ for measurement $S(t)$.

4.2.2. Estimation results: Aggregated substrate concentration measurement. This section presents the estimation results obtained using the hierarchical observer (27) and (29). The trajectories of state variables representing $X(t)$, $DO(t)$, and $X_\mathrm{r}(t)$, and the kinetic function $\mu(t)$ which were generated by the model (22) and their estimates from the AO (27) and the STSMO (29) are shown in Figs. 11, 12, 13 and 14, respectively.

When analysing the trajectories shown in Figs. 11–13, it can be noticed that, like in Section 4.2.1, the estimation performance for the state variable representing the concentration of dissolved oxygen is very high practically from the beginning of the simulation, while for the state variables representing the concentrations of biomass this performance is satisfactory after about 80 [h]. Compared with the case previously considered, this increase in the convergence time of the estimation trajectories to the real values of state variables is due to the features of the measurement used (aggregated substrate concentration—see Fig. 6). However, it is worth noting that, also in this case, the rate of convergence can be increased by selecting the initial conditions appropriately—see the trajectories with the dotted line in Figs. 11 and 13. In turn, the behaviour of the original and reconstructed kinetic function (Fig. 14) shows that the tracking of the unknown kinetic function using two pseudo-measurements is also satisfactory.

5. Conclusions

In this paper, the problem of estimation of unmeasured state variables and an unknown kinetic function for biochemical processes modelled as a continuous stirred tank reactor was investigated. In detail, a novel hierarchical observer which unites the adjusted asymptotic observer and the adopted super-twisting sliding mode observer was devised to produce stable estimates of the unmeasured state variables and the unknown kinetic function. The designed asymptotic observer allows reconstructing the unmeasured state variables in the presence of uncertainties in the dynamics introduced by the unknown kinetic function. Moreover, this observer takes into account several input signals. Then, the generated estimates of the unmeasured state variables constituting the pseudo-measurements are used together with the available direct measurements by the super-twisting sliding mode observer to estimate the unknown kinetic function. In this way, the estimation process is completed and provides full information about the unknown variables. The global asymptotic convergence of the produced estimates or the asymptotic

stability of the estimation errors was rigorously proved using the methodology associated with linear parameter-varying systems and sliding mode regimes. The developed hierarchical observer was implemented in the Matlab/Simulink environment, and its performance was verified by simulation. Simulation experiments were carried out for various measured outputs that may be available in the water resource recovery facility. A satisfactory performance of the generated estimates was obtained, which confirms the high effectiveness of the devised hierarchical observer.

The obtained estimation results can be applied both in state monitoring systems for processes in water resource recovery facilities, and in advanced control algorithms for these plants. Future research will aim at using the developed approach for more sophisticated models of biochemical processes, in general, in urban water systems.

Acknowledgment

The financial support of this research from the Gdańsk University of Technology within the DEC-/2020/IDUB/I.3.3 grant under the Argentum Triggering Research Grants *Excellence Initiative—Research University* program is gratefully acknowledged.

References

Alcaraz-González, V., Harmand, J., Rapaport, A., Steyer, J.P., González-Alvarez, V. and Pelayo Ortiz, C. (2005). Application of a robust interval observer to an anaerobic digestion process, *Developments in Chemical Engineering & Mineral Processing* **13**(3–4): 267–278, DOI: 10.1002/apj.5500130308.

Bárzaga-Martell, L., Duarte-Mermoud, M.A., Ibáñez Espinel, F., Gamboa-Labbé, B., Saa, P.A. and Pérez-Correa, J.R. (2021). A robust hybrid observer for monitoring high-cell density cultures exhibiting overflow metabolism, *Journal of Process Control* **104**: 112–125, DOI: 10.1016/j.jprocont.2021.06.006.

Bastin, G. and Dochain, D. (1990). *On-Line Estimation and Adaptive Control of Bioreactors*, Elsevier, Amsterdam.

Bogaerts, P. (1999). A hybrid asymptotic Kalman observer for bioprocesses, *Bioprocess Engineering* **20**: 249–255, DOI: 10.1007/s004490050587.

Bogaerts, P. and Coutinho, D. (2014). Robust nonlinear state estimation of bioreactors based on H^{∞} hybrid observers, *Computers & Chemical Engineering* **60**: 315–328, DOI: 10.1016/j.compchemeng.2013.09.013.

Bogaerts, P. and Hanus, R. (2001). On-line state estimation of bioprocesses with full horizon observers, *Mathematics and Computers in Simulation* **56**(4–5): 425–441.

Bogaerts, P. and Vande Wouwer, A. (2003). Software sensors for bioprocesses, *ISA Transactions* **42**(4): 547–558, DOI: 10.1016/S0019-0578(07)60005-6.

Boyd, S., El Ghaoui, L., Feron, E. and Venkataramanan, B. (1994). *Linear Matrix Inequalities in System and Control Theory*, SIAM, Philadelphia.

Coutinho, D., Vargas, A., Feudjio, C., Benavides, M. and Vande Wouwer, A. (2019). A robust approach to the design of super-twisting observers—Application to monitoring microalgae cultures in photo-bioreactors, *Computers & Chemical Engineering* **121**: 46–56, DOI: 10.1016/j.compchemeng.2018.07.006.

Czyżniewski, M. and Łangowski, R. (2022a). An observability and detectability analysis for non-linear uncertain CSTR model of biochemical processes, *Scientific Reports* **12**: 22327, DOI: 10.1038/s41598-022-26656-3.

Czyżniewski, M. and Łangowski, R. (2022b). A robust sliding mode observer for non-linear uncertain biochemical systems, *ISA Transactions* **123**: 25–45, DOI: 10.1016/j.isatra.2021.05.040.

Czyżniewski, M., Łangowski, R. and Piotrowski, R. (2023). Respiration rate estimation using non-linear observers in application to wastewater treatment plant, *Journal of Process Control* **124**: 70–82, DOI: 10.1016/j.jprocont.2023.02.00.

De Battista, H., Picó, J., Garelli, F. and Navarro, J.L. (2012). Reaction rate reconstruction from biomass concentration measurement in bioreactors using modified second-order sliding mode algorithms, *Bioprocess and Biosystems Engineering* **35**: 1615–1625, DOI: 10.1007/s00449-012-0752-y.

De Battista, H., Picó, J., Garelli, F. and Vignoni, A. (2011). Specific growth rate estimation in (fed-)batch bioreactors using second-order sliding observers, *Journal of Process Control* **21**(7): 1049–1055, DOI: 10.1016/j.jprocont.2011.05.008.

Dewasme, L., Goffaux, G., Hantson, A.-L. and Vande Wouwer, A. (2013). Experimental validation of an extended Kalman filter estimating acetate concentration *in E. coli* cultures, *Journal of Process Control* **23**(2): 148–157, DOI: 10.1016/j.jprocont.2012.09.004.

Dewasme, L., Sbarciog, M., Rocha-Cózatl, E., Haugen, R. and Vande Wouwer, A. (2019). State and unknown input estimation of an anaerobic digestion reactor with experimental validation, *Control Engineering Practice* **85**: 280–289, DOI: 10.1016/j.conengprac.2019.02.003.

Dewasme, L. and Vande Wouwer, A. (2020). Experimental validation of a full-horizon interval observer applied to hybridoma cell cultures, *International Journal of Control* **93**(11): 2719–2728, DOI: 10.1080/00207179.2019.1608372.

Dochain, D. and Perrier, M. (2002). A state observer for (bio)processes with uncertain kinetics, *Proceedings of the 2002 American Control Conference, Anchorage, USA*, pp. 2873–2878, DOI: 10.1109/ACC.2002.1025225.

Dochain, D. and Vanrolleghem, P.A. (2001). *Dynamical Modelling and Estimation in Wastewater Treatment Processes*, IWA Publishing, London.

Elsheikh, M., Hille, R., Tatulea-Codrean, A. and Krämer, S. (2021). A comparative review of multi-rate moving horizon estimation schemes for bioprocess applications, *Computers & Chemical Engineering* **146**: 107219, DOI: 10.1016/j.compchemeng.2020.107219.

Farza, M., Busawon, K. and Hammouri, H. (1998). Simple nonlinear observers for on-line estimation of kinetic rates in bioreactors, *Automatica* **34**(3): 301–318, DOI: 10.1016/S0005-1098(97)00166-0.

Fridman, L., Moreno, J.A. and Iriarte, R. (2011). *Sliding Modes After the First Decade of the 21st Century*, Springer, Berlin.

Garcia-Ochoa, F. and Gomez, E. (2009). Bioreactor scale-up and oxygen transfer rate in microbial processes: An overview, *Biotechnology Advances* **27**(2): 153–176, DOI: 10.1016/j.biotechadv.2008.10.006.

Ha Hoang, N., Couenne, F., Le Gorrec, Y., Chen, C.L. and Ydstie, B.E. (2013). Passivity-based nonlinear control of CSTR via asymptotic observers, *Annual Reviews in Control* **37**(2): 278–288, DOI: 10.1016/j.arcontrol.2013.09.007.

Hadj-Sadok, M.Z. and Gouzé, J.-L. (2005). Estimation of uncertain models of activated sludge processes with interval observers, *Journal of Process Control* **11**(3): 299–310, DOI: 10.1016/S0959-1524(99)00074-8.

Henze, M., Gujer, W., Mino, T. and Van Loosdrecht, M. (2000). *Activated Sludge Models ASM1, ASM2, ASM2d and ASM3*, IWA Publishing, London.

Hulhoven, X., Vande Wouwer, A. and Bogaerts, P. (2006). Hybrid extended Luenberger-asymptotic observer for bioprocess state estimation, *Chemical Engineering Science* **61**(21): 7151–7160.

Hulhoven, X., Vande Wouwer, A. and Bogaerts, P. (2008). State observer scheme for joint kinetic parameter and state estimation, *Chemical Engineering Science* **63**(19): 4810–4819.

Ilchmann, A., Owens, D.H. and Prätzel-Wolters, D. (1987). Sufficient conditions for stability of linear time-varying systems, *Systems & Control Letters* **9**(2): 157–163, DOI: 10.1016/0167-6911(87)90022-3.

Jenkins, B.M., Annaswamy, A.M., Lavretsky, E. and Gibson, T.E. (2018). Convergence properties of adaptive systems and the definition of exponential stability, *SIAM Journal on Control and Optimization* **56**(4): 2463–2484, DOI: 10.1137/15M1047805.

Junosza-Szaniawski, K., Nogalski, D. and Rzążewski, P. (2022). Exact and approximation algorithms for sensor placement against DDoS attacks, *International Journal of Applied Mathematics and Computer Science* **32**(1): 35–49, DOI: 10.34768/amcs-2022-0004.

Khalil, H.K. (2002). *Nonlinear Systems, 3rd Edition*, Prentice-Hall, Inc., Upper Saddle River.

Lafont, F., Pessel, N., Balmat, J.-F. and Gauthier, J.-P. (2014). Unknown-input observability with an application to prognostics for waste water treatment plants, *European Journal of Control* **20**(2): 95–103, DOI: 10.1016/j.ejcon.2014.01.002.

Łangowski, R. and Brdys, M.A. (2017). An interval estimator for chlorine monitoring in drinking water distribution systems under uncertain system dynamics, inputs and chlorine concentration measurement errors, *International Journal of Applied Mathematics and Computer Science* **27**(2): 309–322, DOI: 10.1515/amcs-2017-0022.

Łangowski, R. and Brdys, M.A. (2018). An optimised placement of the hard quality sensors for a robust monitoring of the chlorine concentration in drinking water distribution systems, *Journal of Process Control* **68**: 52–63, DOI: 10.1016/j.jprocont.2018.04.007.

Lemesle, V. and Gouzé, J.-L. (2005). Hybrid bounded error observers for uncertain bioreactor models, *Bioprocess and Biosystems Engineering* **27**(5): 311–318.

Lindberg, C.F. (1997). *Control and Estimation Strategies Applied to the Activated Sludge Process*, PhD thesis, Uppsala University, Uppsala.

López-Caamal, F. and Moreno, J.A. (2016). Unmeasured concentrations and reaction rates estimation in CSTRs, *IFAC-PapersOnLine* **49**(7): 224–229, DOI: 10.1016/j.ifacol.2016.07.262.

López-Estrada, F.-R., Ponsart, J.-C., Theilliol, D., Astorga-Zaragoza, C.-M. and Camas-Anzueto, J.-L. (2015). Robust sensor fault estimation for descriptor-LPV systems with unmeasurable gain scheduling functions: Application to an anaerobic bioreactor, *International Journal of Applied Mathematics and Computer Science* **25**(2): 233–244, DOI: 10.1515/amcs-2015-0018.

Moreno, J.A. (2012). Lyapunov approach for analysis and design of second order sliding mode algorithms, *in* L. Fridman *et al.* (Eds), *Sliding Modes After the First Decade of the 21st Century: State of the Art*, Springer, Berlin/Heidelberg, pp. 113–149, DOI: 10.1007/978-3-642-22164-4_4.

Moreno, J.A. and Dochain, D. (2008). Global observability and detectability analysis of uncertain reaction systems and observer design, *International Journal of Control* **81**(1): 1062–1070, DOI: 10.1080/00207170701636534.

Moreno, J.A. and Mendoza, I. (2014). Application of super-twisting-like observers for bioprocesses, *13th International Workshop on Variable Structure Systems (VSS), Nantes, France*, pp. 1–6, DOI: 10.1109/VSS.2014.6881102.

Moreno, J.A. and Osorio, M. (2012). Strict Lyapunov functions for the super-twisting algorithm, *IEEE Transactions on Automatic Control* **57**(4): 1035–1040, DOI: 10.1109/TAC.2012.2186179.

Moreno, J.A., Rocha-Cózatl, E. and Vande Wouwer, A. (2012). Observability/detectability analysis for nonlinear systems with unknown inputs—Application to biochemical processes, *Preprints of the 2012 20th Mediterranean Conference on Control & Automation (MED), Barcelona, Spain*, pp. 2445–2450, DOI: 10.1109/MED.2012.6265630.

Moshksar, E. and Guay, M. (2014). A geometric approach for adaptive estimation of unknown growth kinetics in bioreactors, *Journal of Process Control* **24**(10): 1496–1503, DOI: 10.1016/j.jprocont.2014.06.017.

Nuñez, S., De Battista, H., Garelli, F., Vignoni, A. and Picó, J. (2013). Second-order sliding mode observer for multiple kinetic rates estimation in bioprocesses, *Control Engineering Practice* **21**(9): 1259–1265, DOI: 10.1016/j.conengprac.2013.03.003.

Oubabas, H., Djennoune, S. and Bettayeb, M. (2018). Interval sliding mode observer design for linear and nonlinear systems, *Journal of Process Control* **61**: 12–22, DOI: 10.1016/j.jprocont.2017.10.004.

Piotrowski, R., Sawicki, H. and Żuk, K. (2021). Novel hierarchical nonlinear control algorithm to improve dissolved oxygen control in biological WWTP, *Journal of Process Control* **105**: 78–87, DOI: 10.1016/j.jprocont.2021.07.009.

Reis de Souza, A., Gouzé, J.-L., Efimov, D. and Polyakov, A. (2020). Robust adaptive estimation in the competitive chemostat, *Computers & Chemical Engineering* **142**: 107030, DOI: 10.1016/j.compchemeng.2020.107030.

Rodríguez, A., Quiroz, G., Femat, R., Méndez-Acosta, H.O. and de León, J. (2015). An adaptive observer for operation monitoring of anaerobic digestion wastewater treatment, *Chemical Engineering Journal* **269**: 186–193, DOI: 10.1016/j.cej.2015.01.038.

Rueda-Escobedo, J.G., Sbarciog, M., Moreno, J.A., Van Impe, J. and Vande Wouwer, A. (2022). Robust state and input estimation with enhanced convergence rate for monitoring anaerobic digestion, *Journal of Process Control* **117**: 169–180, DOI: 10.1016/j.jprocont.2022.07.014.

Ríos, H., Efimov, D. and Perruquetti, W. (2018). An adaptive sliding-mode observer for a class of uncertain nonlinear systems, *International Journal of Adaptive Control and Signal Processing* **32**(3): 511–527.

Shilov, G. and Chilov, G. (1996). *Elementary Functional Analysis*, Courier Corporation, Moscow.

Srinivasarengan, K., Ragot, J., Aubrun, C. and Maquin, D. (2018). An adaptive observer design approach for a class of discrete-time nonlinear systems, *International Journal of Applied Mathematics and Computer Science* **28**(1): 55–67, DOI: 10.2478/amcs-2018-0004.

Sun, X., Jin, L. and Xiong, M. (2008). Extended Kalman filter for estimation of parameters in nonlinear state-space models of biochemical networks, *PLoS ONE* **3**(11): e3758, DOI: 10.1371/journal.pone.0003758.

Taylor, J.A., Rapaport, A. and Dochain, D. (2022). A sequential convex moving horizon estimator for bioprocesses, *Journal of Process Control* **116**: 19–24, DOI: 10.1016/j.jprocont.2022.05.012.

Torfs, E., Nicolaï, N., Daneshgar, S., Copp, J.B., Haimi, H., Ikumi, D., Johnson, B., Plosz, B.B., Snowling, S., Townley, L.R., Valverde-Pérez, B., Vanrolleghem, P.A., Vezzaro, L. and Nopens, I. (2022). The transition of WRRF models to digital twin applications, *Water Science and Technology* **85**(10): 2840–2853, DOI: 10.2166/wst.2022.107.

Tuveri, A., Holck, H.E., Nakama, C.S.M., Matias, J., Jäschke, J., Imsland, L. and Bar, N. (2022). Bioprocess monitoring: A moving horizon estimation experimental application, *IFAC-PapersOnLine* **55**(7): 222–227, DOI: 10.1016/j.ifacol.2022.07.448.

Ujazdowski, T., Zubowicz, T. and Piotrowski, R. (2023). A comprehensive approach to SBR modelling for monitoring and control system design, *Journal of Water Process Engineering* **53**: 103774, DOI: 10.1016/j.isatra.2021.05.040.

Yin, X. and Liu, J. (2017). Distributed moving horizon state estimation of two-time-scale nonlinear systems, *Automatica* **79**: 152–161, DOI: 10.1016/j.automatica.2017.01.023.

Zhou, B. (2016). On asymptotic stability of linear time-varying systems, *Automatica* **68**: 266–276, DOI: 10.1016/j.automatica.2015.12.030.

Mateusz Czyżniewski received his MSc degree (Hons.) in control engineering from the Faculty of Electrical and Control Engineering at the Gdańsk University of Technology in 2019. Since then he has been a PhD student at the Gdańsk University of Technology in the field of control engineering. His research interests involve advanced non-linear control theory, mathematical modelling of dynamical systems, and robust estimation and monitoring methods.

Rafał Łangowski received his MSc and PhD degrees (Hons.) in control engineering from the Faculty of Electrical and Control Engineering at the Gdańsk University of Technology in 2003 and 2015, respectively. From 2007 to 2014, he held the positions of a specialist as well as a manager at ENERGA, one of the biggest energy enterprises in Poland. He is currently an assistant professor with the Department of Intelligent Control and Decision Support Systems at the Gdańsk University of Technology. His research interests involve mathematical modelling and identification, estimation methods, especially state observers, and monitoring of large-scale complex systems.

Appendix

Analysis of the boundedness of the internal dynamics matrix

This section outlines the key issues related to the uniform boundedness of matrices $\boldsymbol{A}(\boldsymbol{u}(t))$ and $\dot{\boldsymbol{A}}(\boldsymbol{u}(t))$ referred to in Section 3.1. For the sake of deriving the constant parameter γ, a matrix norm is defined as the Frobenius matrix norm (Shilov and Chilov, 1996). This approach is based on solving an appropriate optimisation task concerning the objective function defined as

$$\begin{aligned}&\|\boldsymbol{A}(\boldsymbol{u}(t))\|_2\\&\triangleq \max\Big\{\Big[\sum_{i_\mathrm{A}=1}^{n}\sum_{j_\mathrm{A}=1}^{n} A_{i_\mathrm{A}j_\mathrm{A}}^2(\boldsymbol{u}(t))\Big]^{\frac{1}{2}}: \boldsymbol{u}(t)\in\mathbb{U}_\mathrm{p}\Big\}\\&\leq \gamma,\end{aligned} \tag{A1}$$

where $i_{\mathrm{A}}, j_{\mathrm{A}} = \overline{1,n}$.

Due to the fact that the input vector $\boldsymbol{u}(t)$ is bounded and continuous (see Assumption 4), the norm defined in (A1) can be easily calculated. To accomplish the constant parameter δ, the matrix norm is again defined as the Frobenius matrix norm (A1). This approach is based on solving the following optimisation task:

$$\begin{aligned}\left\|\dot{\boldsymbol{A}}(\boldsymbol{u}(t))\right\|_2 &= \left\|\partial_{\boldsymbol{u}}\boldsymbol{A}(\boldsymbol{u}(t))\left[\mathbf{1}_{(\mathrm{n}\times 1)}\otimes\dot{\boldsymbol{u}}(t)\right]\right\|_2\\ &\le \left\|\partial_{\boldsymbol{u}}\boldsymbol{A}(\boldsymbol{u}(t))\right\|_2\left\|\mathbf{1}_{(\mathrm{n}\times 1)}\otimes\dot{\boldsymbol{u}}(t)\right\|_2\\ &\le \left\|\partial_{\boldsymbol{u}}\boldsymbol{A}(\boldsymbol{u}(t))\right\|_2\left\|\dot{\boldsymbol{u}}(t)\right\|_2\\ &\le \left\|\partial_{\boldsymbol{u}}\boldsymbol{A}(\boldsymbol{u}(t))\right\|_2\overline{\boldsymbol{u}}_{\mathrm{d}} \le \delta,\end{aligned}$$

$$\dim\left(\partial_{\boldsymbol{u}}\boldsymbol{A}(\boldsymbol{u}(t))\right) = n\times(np), \tag{A2}$$

$$\dim\left(\mathbf{1}_{(\mathrm{n}\times 1)}\otimes\dot{\boldsymbol{u}}(t)\right) = (np)\times 1,$$

$$\begin{aligned}&\left\|\partial_{\boldsymbol{u}}\boldsymbol{A}(\boldsymbol{u}(t))\right\|_2\\ &\quad\triangleq \max\Big\{\Big[\sum_{i_{\mathrm{dA}}=1}^{n}\sum_{j_{\mathrm{dA}}=1}^{np}\partial_{\boldsymbol{u}}A^2_{i_{\mathrm{dA}}j_{\mathrm{dA}}}(\boldsymbol{u}(t))\Big]^{\frac{1}{2}}\Big\},\\ &\quad\boldsymbol{u}(t)\in\mathbb{U}_{\mathrm{p}},\quad i_{\mathrm{dA}} = \overline{1,n},\quad j_{\mathrm{dA}} = \overline{1,np},\end{aligned}$$

where $\otimes$ denotes the Kronecker product (Shilov and Chilov, 1996; Khalil, 2002), and $\overline{\boldsymbol{u}}_{\mathrm{d}} \in \mathbb{R}^{\mathrm{n}}_{+}$ is the vector composed of particular inputs $\overline{u}_{\mathrm{d}_{i_{\mathrm{p}}}}$ introduced in Assumption 4.

Knowing that matrix $\boldsymbol{A}(\boldsymbol{u}(t))$ is $n\times n$-dimensional, its Jacobi matrix with respect to $\boldsymbol{u}(t)$ must be $n\times(np)$-dimensional. Therefore, the $\dot{\boldsymbol{u}}(t)$ associated Kronecker multiplication must be introduced. Next, the Frobenius matrix norm is assessed by using the Schwartz inequality for vectors and matrices (Shilov and Chilov, 1996). Since the input vector $\boldsymbol{u}(t)$ is bounded and continuous, the norm defined in (5) can be easily calculated.

Received: 22 August 2023
Revised: 8 December 2023
Accepted: 8 December 2023